The Use of Proton Exchange Membrane Fuel Cells (PEMFCs) in Refrigerated Transport for the Frozen Food Supply Chain

Balraj Singh Ghataore

[redacted]

A Thesis submitted to The University of Birmingham for the degree of

Master of Research (MRes)

The Centre for Hydrogen and Fuel Cell Research
PEM Fuel Cell Research group
School of Chemical Engineering
College of Engineering & Physical Sciences
The University of Birmingham

Abstract

The transport of food is a vital element in the food supply chain. However, due to changes in consumer buying habits and the decline of the agricultural industry in the EU, there is an increasing dependency on importing and transporting food over long distances; this requires Heavy Goods Vehicles (HGV), large marine vehicles and aircraft. Over the last 30 years, the increased number of HGVs in this sector has caused an 84.5% increase in emissions, energy consumption and fuel consumption [1]. With global pressures such as climate change and the limited future of fossil fuels, such an increase in activity means that there is a need to seek alternate solutions for refrigerated road delivery vehicles.

Hydrogen fuel cells have been used effectively in automotive vehicles, Combined Heat and Power (CHP) units and refrigeration systems. Proton Exchange Membrane Fuel Cells (PEMFCs) are ideal for automotive applications due to the continually reducing cost, high energy density and solid state polymer electrolyte membrane. PEMFC hybrid vehicle systems have been developed with success with low maintenance due to few moving parts. In addition the solid state electrolyte in these fuel cells enables dense packing of these cells to provide high power densities. PEMFCs also do not have issues of corrosion caused by aqueous acidic and alkaline electrolytes. The use of such electrolytes has seen many issues in vehicles such as the GM Electrovan produced in 1966 [2].

This thesis reviews the current literature and the use of fuel cells in refrigerated transport. The benefits of using a fuel cell in a hybridised layout for both traction and onboard refrigeration have been modelled. The refrigeration model in this thesis explores the use of sorption refrigeration by using the waste heat produced by the fuel cell reaction. To produce subzero

temperatures, ammonia sorption refrigeration systems are required which require high generator temperatures. Since the operation temperature of PEMFCs is low, this thesis analyses the use of sorption systems which are capable of producing temperatures above 0°C with lower generator temperatures in a dual stage sorption-vapour compression refrigeration system. This thesis concludes that using such systems will reduce the energy and cost to power a compressor in a vapour compression refrigeration system.

The vehicle system has also been modelled highlight the effect of hybridisation on vehicle weight. The model shows that a hybridised vehicle has the potential to save 30% of energy during the New European Drive Cycle (NEDC). This model also shows that hybridisation of 0.1 in Heavy Goods Vehicles (HGVs) can result in an increase in energy consumption compared with pure fuel cell vehicles. In addition as vehicle weight increases, the fuel cell increasingly becomes the primary energy source during the NEDC and can potentially operate inefficiently during urban driving. Further work is needed in this area to quantify the efficiencies and therefore the fuel consumption of fuel cell hybrid HGVs. The costs have also been modelled in this thesis which further highlights the benefits of using fuel cells in a hybridised layout.

Contents

List of Figures

List of Tables

1. Introduction

Over the last 50 years, our buying habits and demands for food have changed. This has had a direct impact on global food production and transportation which has lead to an increase in energy consumption in this sector. The increase in food demand and the reduction of agriculture in European countries has forced globalisation of this sector resulting in the increasing need for mass transport vehicles such as refrigerated heavy goods vehicles (HGVs), marine vessels and aircraft [1].

Between 1978 and 2005, HGV transportation has increased by 23% with an average increase in distance travelled of 50% [1]. This increase in food miles translates to an increase of 84.5% in energy consumption, fuel consumption and emissions over this period [1].

In addition to environmental concerns, the future supply of fuel is also a concern. In 2010, the proven global oil reserves stood at 188.8 billion tonnes with 4028.1 million tonnes being consumed during 2010 [3]. Using proven oil reserves and assuming that fuel consumption will remain at the same rate as 2010, a 45.9 year oil supply remains from the beginning of 2012.

In addition to environmental concerns and the rapid depletion of fossil fuel reserves, businesses are also coming under pressure to reduce emissions from business activities, including those involving transportation. In many countries across Europe, road tax is dependent on the vehicle carbon emissions. High polluting HGVs can pay up to £1850 per year in the UK, which can have a significant impact on profits [4]. This figure is reduced to £1350 per year [4] for vehicles which incorporate low carbon emission technology.

Vehicle emissions also can limit deliveries. In some urban areas across the EU, in an attempt to reduce congestion and emissions there are an increasing number of low emission zones (LEZs). Currently there are hundreds of LEZs across Europe which all affect HGVs above 3.5 tonnes [5]. A majority of these zones operate 24 hours a day and the scheme mainly targets particulates (common in diesel vehicles), nitrous oxides and indirectly produced ozone. There is a focus on these emissions as poor air quality is responsible for 310,000 premature deaths in Europe [5].

Such zones have proven to be very effective in reducing emissions and congestion, however deliveries in these areas may be affected as vehicles that do not comply with the Euro standard stated for the LEZ may not enter [5]. Furthermore, although internal combustion engine (ICE) technology for commercial vehicles has seen major improvements in fuel consumption (directly proportional to emissions) over the last 45 years, ICE technology has not seen major improvements over the last 15 years (Figure 1) [6]. Therefore there is a need to seek alternative traction and cabin temperature control solutions in order to reduce emissions of food delivery vehicles.

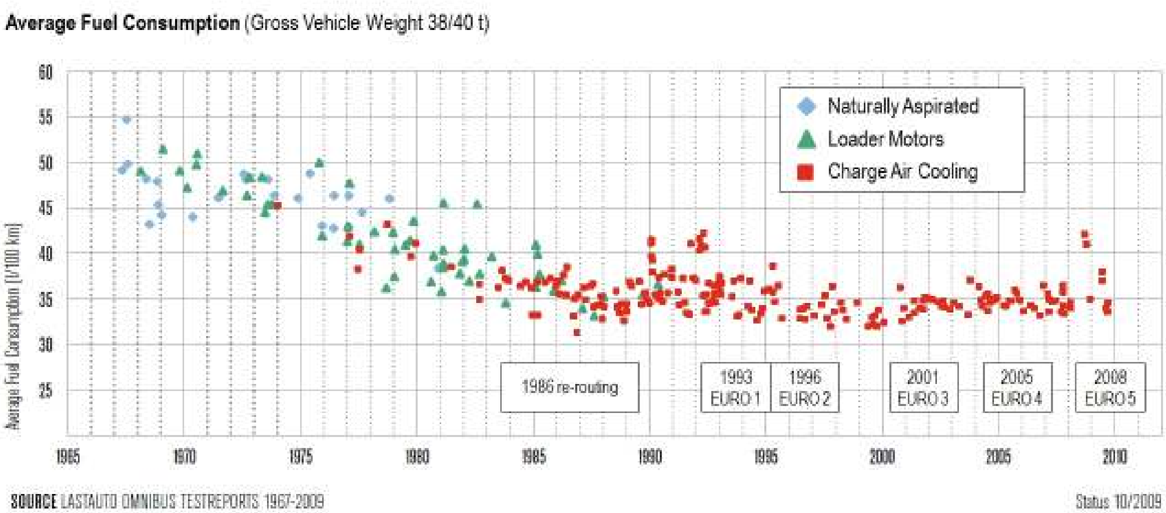

Figure 1 - Graph showing advances in ICE technology in HGVs and the average fuel consumption [6]

As LEZ have spread across Europe, low noise zones have been proposed specifically aimed at reducing traffic noise. Restrictions have already been introduced in the Netherlands (PIEK standard) that limits noise between the hours of 19:00 and 07:00 to less than 60dB for vehicles up to 7.5 tonnes [7]. As current refrigerated vehicles use diesel engines to run noisy vapour compression systems, future noise legislation may affect refrigerated deliveries which are normally conducted at night. Low noise units which comply with the PIEK standard have been produced by Carrier Transicold (modified Vector unit) and Thermoking (SLX Whisper Unit) [8, 9].

1.1Refrigeration

The first modern refrigerator was constructed and patented by Jacob Perkins in 1834 [10, 11] and forms the foundation for current vapour compressor (VC) systems shown in Figure 2. In these systems, the refrigerant is circulated by a mechanical compressor which requires work/power input. The compressor also provides the increase in pressure so heat is rejected at the condenser of the system.

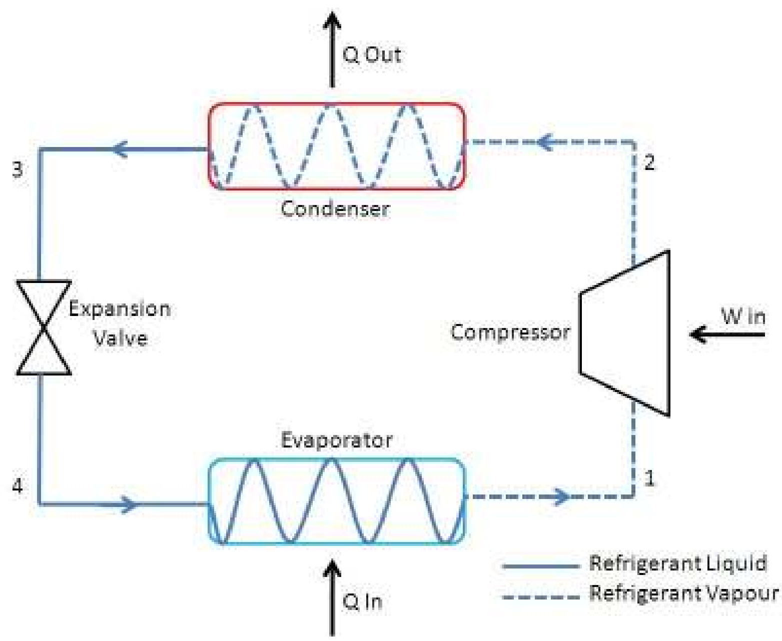

Figure 2 - Schematic of Vapour Compression Refrigeration System

VC refrigeration is a very mature technology and there are a wide range of methods to drive the compressor in these systems which has meant that these refrigeration systems have been the primary choice in vehicle refrigeration.

Other systems can provide refrigeration; the most common among other technologies is sorption refrigeration (adsorption and absorption). Like VC systems, these systems use the same refrigeration cycle, however the mechanical compressor is replaced with a thermal compressor. Figure 3 shows a schematic of a sorption systems and the construction of the thermal compressor.

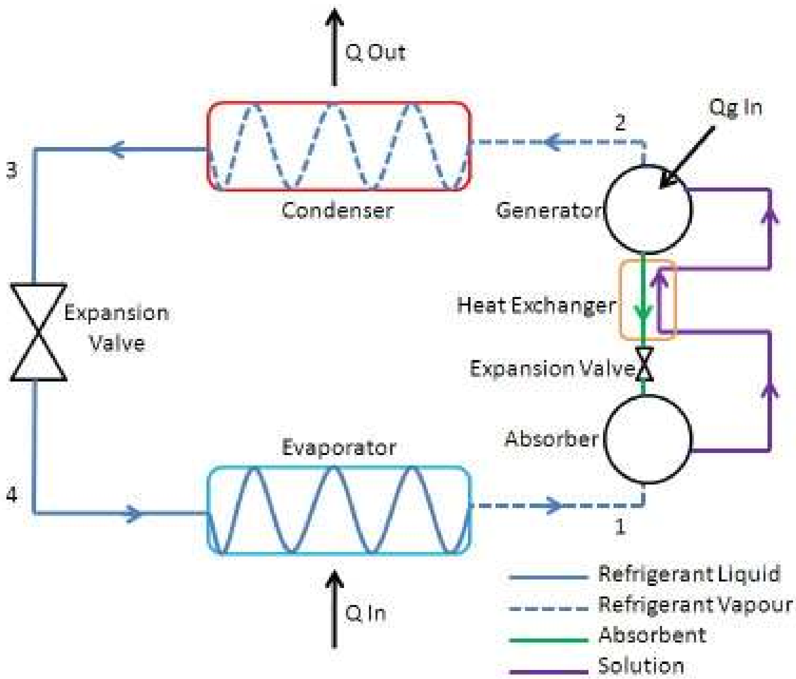

Figure 3 - Schematic of Absorption Refrigeration System

In sorption systems, a solid (in adsorption systems) or an additional liquid (in absorption systems) known as an absorbent is used. Since these systems use a thermal compressor, heat from many applications can be used such as solar, engine exhaust heat, electric heaters, heat from combustion processes and waste heat from fuel cells. Sorption systems are also simpler in construction and have no complex moving parts and therefore need less maintenance and no lubrication is required. In addition, these systems are quiet in operation and can provide greater overall system efficiency if waste heat from processes is used.

Absorption refrigeration equipment can be broadly based on the refrigerant it uses, water or ammonia [12]. Water systems use lithium bromide (LiBr) as an absorbent and are used in large commercial chillers where temperatures above 0°C are required. Ammonia systems use water as an absorbent and these systems are commonly used in domestic refrigerators, residential chillers and large industrial refrigeration systems where a temperature below 0°C is required [12]. Typical adsorption systems use water as a refrigerant and solid silica gel as an absorbent and are ideal for temperature requirements above 0°C [13].

Although sorption based systems have drawbacks such as high weight, large volume, higher cost and low Coefficient of Performance (COP) compared to the more popular vapour compression systems [12, 14], sorption systems have the ability to use high and low grade heat. Adsorption systems benefit from the key advantages of all sorption systems stated. In addition to these advantages, due to the solid sorbent, there is no need to circulate refrigerant/sorbent solution like in absorption systems. Sorption systems are significantly larger and heavier that VC systems which is an issue in refrigerated transport.

For ice cream storage and transportation, a maximum product temperature of -18°C is a compulsory requirement set out in the EU Directive for frozen foods [15]. To ensure this temperature is maintained and due to current supply chain practices, a 2°C buffer is implemented at each stage of the supply chain (Table 3). This means that for the transport of frozen foods, a minimum product temperature of -22°C is required to ensure that there is no spoilage of product during loading and unloading. This means that for frozen food applications, water – ammonia absorption systems are the only viable refrigeration solution due to the temperatures these systems can produce. However, water – ammonia systems require temperatures of approximately 220°C to provide a COP of below 0.5 to produce the freezing temperatures required to store frozen products [12, 16].

In commercial water – silica gel adsorption systems, temperatures at the generator in the region of 50 – 90°C are required which provide a COP of approximately 0.7 and produce temperatures above 0°C [14]. In recent years, Zeolith has been used as an alternative to silica by some manufacturers, however these systems produce similar COP and evaporator temperatures as silica systems which do not meet the requirements for frozen applications [17].

Research is being conducted to produce sorption systems which provide greater COP and lower temperatures of around -25°C whilst taking advantage of the possible use of low grade heat [14].

Other refrigeration technologies are highlighted in Table 1. These refrigeration systems have relatively low COP and have greater cost compared with VC systems. Air cycle and ejector refrigeration have been highlighted by Tassou et al. [14] as having potential to be used in onboard refrigeration. However off the shelf systems for food applications are not available and these systems have low COP compared with current VC systems.

Table 1 – Characteristics of emerging refrigeration technologies [14]

Refrigeration technology	State of development	Cooling capacity of presently available R&D systems	Efficiency/COP of presently available or R&D systems
Tri-generation	Large capacity bespoke systems available. Smaller capacity integrated systems at R&D stage	12kW - MW	Overall system efficiency 65 - 90%. Refrigeration system COP: 0.3 at -50C at 12C
Air cycle	Bespoke systems available	11kW - 700kW	0.4 - 0.7
Ejector	Bespoke steam ejector systems available	Few kW to 60MW	Up to 0.3
Stirling	small capacity systems available. Large systems are R&D stage	15 - 300W	1.0 - 3.0
Thermoelectric	Low cost low efficiency systems available	Few Watts to 20kW	0.6 at 0C
Thermoacoustic	R&D stage, predicted commercialisation 5 - 10 years	Few watts to kW capacity	Up to 1.0
Magnetic	R&D stage, predicted commercialisation 10+ years	Up to 540W	at room temperature

1.2 Agreement Specifying the Performance of Refrigerated Vehicles

Food transportation must ensure that the quality and safety of produce is maintained with minimum losses. The Agreement Transports Périssables (ATP) is an agreement for the International Carriage of Perishable Foodstuffs and was drafted by the Inland Transport Committee of the United Nations Economic Committee for Europe in 1970-71 [18]. This agreement sets out a common international standard for the storage and transportation of perishable food. For road vehicles in the UK, refrigerated vehicles are tested to ensure that the correct temperatures are maintained and vehicle insulation is fit for purpose. Vehicles that pass vehicle testing and meet the minimum requirements are then certified to transport food products within the country and internationally [18]. All signatories of the ATP must meet the standard in order to transport produce internationally. If food it being transported within the country only, ATP certification is not required for most countries, however certification is required for France, Spain, Italy and Portugal [18].

The ATP categorises all insulated bodies including road vehicles by a test known as the Cambridge K test [18] which calculates an overall insulation heat transfer coefficient (K) shown in [18, 19].

$$K = \frac{W}{S\Delta T} \qquad \text{(Equation 1)}$$

Where: W is the cooling capacity required to maintain a constant temperature difference, ΔT, between the outside and interior of the vehicle of mean surface area, S, which is calculated from:

$$S = \sqrt{S_i S_e} \qquad \text{(Equation 2)}$$

Where S_i, S_e are the inside and outside surface areas of the vehicle.

The ATP specifies two categories for mechanically insulated vehicles: normally insulated and heavily insulated. Details of each category are listed in Table 2; it can be seen that for the delivery of frozen products (-22°C) [15], the heavily insulated category requirements must be fulfilled.

Table 2 - ATP Classification for Insulation of mechanical refrigerated equipment [18]

	K Coefficient ($Wm^{-2}K^{-1}$)	Operating Temperatures (°C)	ATP Classification
Normal Insulation	0.7 – 0.4	0 to +12	FNA
Heavy insulation,	< 0.4	-20 to +12	FRC

In addition to insulation requirements, vehicle refrigeration equipment must be approved. The agreement sets out requirements for refrigeration units which are installed or uninstalled on a vehicle. If the unit is not installed in the vehicle, the heat extraction must be at least 1.75

times greater than the heat transfer through the walls of the vehicle at an ambient temperature of 30°C to determine the vehicles cooling capacity at the prescribed temperatures [18]. This figure reduced to 1.35 times if the refrigeration unit is combined with insulated volume (installed vehicle units). After these figures are satisfied, refrigeration equipment is categorised at either -20°C, -10°C, 0°C or +12°C [18].

Due to the harsh conditions road vehicles are subject to and deterioration of vehicle insulation and compressor performance over time, ATP certificates are renewed every six years. This can be extended by an addition three years if "in service" tests in conducted [18].

2. Literature Review

2.1 Current Refrigerated Delivery Road Vehicles

There are a wide range of commercial delivery vehicles and selection is dependent on the drive cycle of the vehicle and the loads the vehicle will carry. Figure 4 shows the different types of commercial delivery vehicles.

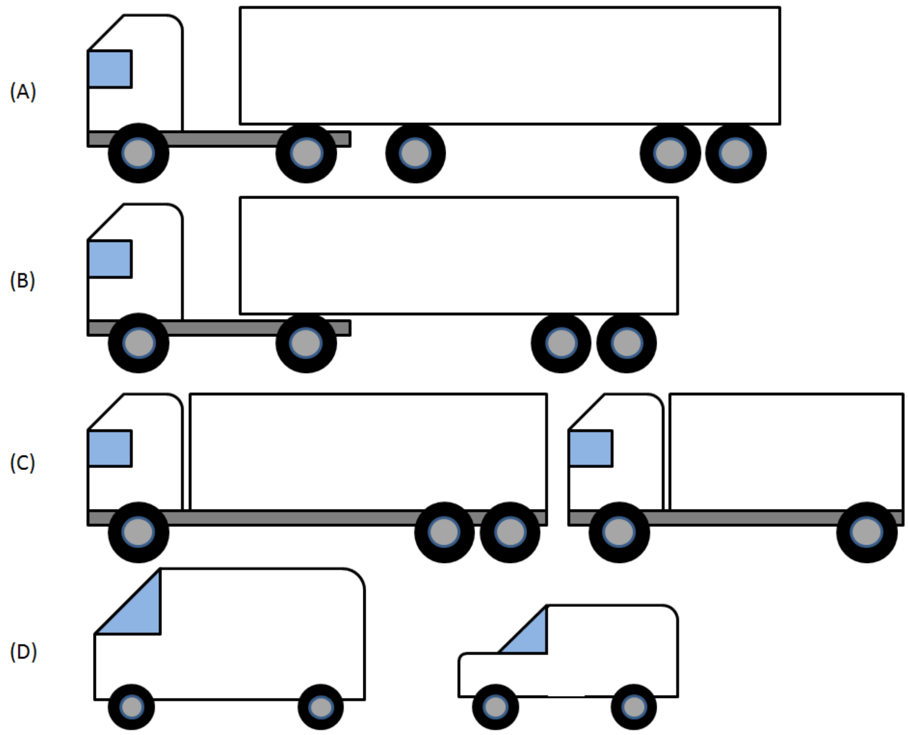

Figure 4 - Different HGVs: (A) Tractor and full trailer with front axle (B) Tractor and semi-tralier without front axle (C) Rigid body (rigid box type) truck (D) Commerical van (panel van)

Space and the ability to carry heavy loads are the fundamental requirements for all delivery transportation. Therefore depending on the drive cycle of a vehicle, the transportation of food is conducted by a range of vehicles from local delivery vans to large articulated trucks. In frozen food transportation, the selection of vehicle and temperature requirements are dependent on the level of transportation in the supply chain as shown in Table 3 – Transport supply chain, vehicles used and temperature requirements [15]Table 3 [15]

Table 3 – Transport supply chain, vehicles used and temperature requirements [15]

Level of Transportation	Description of Transportation Level	Typical Vehicles Used	Average Product Temperature Requirement (°C)	Average Air Temperature Requirement (°C)
Primary Transport	Product moved from primary factory storage to secondary storage (retail distribution centres, wholesalers or local distribution centres)	60 to 40 tonne trucks typically carrying 33 Euro pallets	-22	-25
Secondary Transport	Product moved from secondary cold storage to tertiary cold storage (vending machines, supermarket cold storage and refrigerated cabinets)	Range of vehicles from vans up to 40 tonne trucks. 40 tonne trucks are used for delivery to large outlets such as supermarket cold storage	-20	-22
Tertiary Transport	Home deli very and vending vehicles directly to the consumer	Small to medium panel vans.	-18	-20

The minimum requirement for the storage of all frozen products is set at -18°C by the EU directive for quick frozen foods. At every stage of the frozen food supply chain, a 2°C buffer is implemented to ensure that there is no spoilage of the product during transportation. This is to compensate for product transfer and standing times throughout the supply chain [15].

Tertiary transportation is not usually conducted by Fast Moving Consumer Goods (FMCG) organisations and is usually conducted by third parties and supermarkets. Therefore in FMCG company fleets, small vending vans are fewer in number compared to larger trucks, trailers and large vans. Typical refrigerated vehicles used by such businesses (Primary and secondary transportation) are trailer/semi-trailer and rigid box type vehicles which have a typical size of around [12, 20]:

- 2.4 – 2.6m width
- 3.7 – 4.1m height
- 7.3 – 16.2 m length.

From the typical vehicle sizes, it can be observed that there is a width constraint of approximately 2 euro pallets (1.0 m by 1.2 m) [21]. Assuming ideal product stacking, approximately 100 – 200 mm of space would remain around the load for insulation and air distribution. Due to this constraint, it is very important to keep insulation thickness low. In practice, a compromise has to be achieved between a high volume occupancy and space required for optimal air flow and adequate thermal insulation.

2.1.1 Traction Engines

Transportation vehicles generally use diesel engines due to their torque and economy characteristics [22-24]. Torque on the crankshaft is a good measure of an engines ability to do work [22]. Considering a Compression Ignition (CI) (diesel) and Spark Ignition (SI) (petrol) engine of the same combustion chamber volume, CI engines produce more torque due to the greater compression ratios within the engine resulting in higher pressures within the cylinders [22]. Larger engines also produce more torque and achieve maximum brake torque (MBT) at lower engine speeds compared to smaller engines (Figure 5). MBT at low engine speeds is ideal for long haulage vehicles as high brake torque results in greater ability to do work. Also, lower steady engine speeds result in enhanced fuel economy [22].

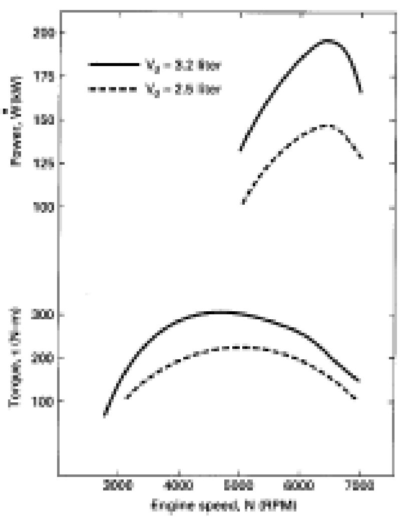

Figure 5 - Graph showing variations of torque and power at varying engine speeds for different engine sizes [22]

Efficiencies of CI engines are also greater than those with SI engines. Combustion efficiency is the fraction of fuel burnt to produce combustion products. SI engines have a combustion efficiency of around 95% whereas CI engines have around 98% efficiency therefore greater fuel economy can be achieved assuming that the swept volumes of both engines are the same [22].

All heat engines including ICEs are limited to the Carnot efficiency which is defined by Equation 3 [19].

$$\eta_{Carnot} = 1 - \frac{T_2}{T_1} \qquad \text{(Equation 3)}$$

Where:

T_1 is the temperature of the heat source (K)

T_2 is the temperature of the heat sink (K)

The Carnot efficiency is the maximum possible thermal efficiency between any two temperatures [19]. For an ICE and assuming an ambient temperature of 25°C (298K) and an adiabatic flame temperature of 2200°C (2473K) [22], a Carnot efficiency of 87.94% can be calculated. The typical thermal efficiency for CI and SI engines at maximum torque is typically around 37% and 28% respectively [25, 26]. This is significantly lower than the maximum efficiency calculated by the Carnot efficiency which is due to irreversibility in real life engine cycles and frictional losses in ICEs.

Due to the higher compression ratio of CI engines (typically between 12-24) compared with SI engines (typically between 8-11), diesel engines have a greater thermal efficiency across a wide power range [22]. Despite their greater efficiencies, diesel engines have disadvantages as they:

- combust fossil fuels which produce greenhouse emissions;
- are noisy in operation;
- are subject to high levels of vibration, which leads to the requirement for regular maintenance and lubrication;
- Emit particulates that have been claimed to be harmful to health [5] but the effects are mitigated by using filters.

The first three issues are also shared with petrol engines.

For all diesel vehicles, for every litre of fuel approximately 2.7kg of carbon dioxide and 9.7kWhr of energy is produced [27]. Table 4 highlights the calculated carbon dioxide emissions and energy consumption for a range of diesel vehicles (without refrigeration units). In refrigerated vehicles, carbon emission and energy consumption are much greater, as is discussed later in this paper.

Table 4 - Calculated Fuel Consumption, Energy Consumption and Carbon Emissions for a Range of Commercial Delivery Vehicles[27, 28]

	Typical Carbon emissions and Energy consumption per 100km					
	Small Van	**Medium Van**	**Large Van**	**Distribution Traffic, Truck**	**Regional Traffic, Truck**	**Long Haulage, Tractor and Trailer**
Payload (tons)	0.77	1.45	2.22	8.5	14	40
Total weight (tons)	2.5	3.3	4.6	14	24	60
Average fuel consumption full load per 100km (litres)	7.2	7.9	8.9	27.5	35	48
CO_2 per 100km full load (kg)	19.44	21.33	24.03	74.25	94.5	129.6
Energy consumption with full load (kWh)	69.84	76.63	86.33	266.75	339.5	465.6
Small Van: Ford Transit 250 SWB (2.2 TDCi 74kW), Medium Van: Ford Transit 330 MWB (2.2TDCi 103kW), Large Van: Ford Transit 460 LWB (2.2 TDCi 114kW)						

2.1.3 Onboard Refrigeration Systems

The purpose of an onboard refrigeration unit is to:

- Ensure that the cold storage temperature is maintained
- Ensure that the cooling capacity is greater than or equal to the effect of transmission load (through the vehicle body and insulation), product load (cooling of the product) and service load (vehicle door openings during deliveries).

2.1.3.1 Onboard Mechanical Refrigeration Systems

VC technology is the most commonly used refrigeration technology in refrigerated transport [12, 20, 29]. VC refrigeration is a mature, reliable technology that allows the compressor to be driven via several options. The compressor drive method can be selected by considering the refrigeration requirement and the drive cycle of the vehicle. During operation, coefficient of performances of around 0.5 – 1.5 are common [20].

Automotive vehicle manufacturers do not produce refrigerated vehicles, refrigeration units are retrofitted. Current onboard mechanical refrigeration systems fall into two broad categories [20, 29].

- ***Direct drive systems*** use the vehicle traction ICE motor to power the compressor of an onboard VC system. These systems place an extra load on the engine which increases fuel consumption and consequently emissions.
- ***Independent systems*** obtain mechanical/electrical power to drive the compressor from methods independent of the traction engine. These systems use a separate ICE motor which provides less power than that of the associated traction ICE motor. The extra ICE motor not only produces extra emissions, but also the addition weight

reduces vehicle performance of the vehicle and increases fuel consumption. These systems can however be run when the traction engine is switched off.

Table 5 lists typical direct drive and independent systems.

Table 5 - Systems Used to Drive On-Board Refrigeration Compressor [12, 20, 29]

		Description	**Type of Vehicle Where system Used**
Direct Drive	Direct belt (V-belt)	Compressor powered directly from the engine crankshaft via a V-belt used to match engine and compressor rotation speed.	Vans. Small trucks.
	Vehicle alternator	Compressor powered by a battery, which is charged via an upgraded alternator. Can operate after the engine is turned off, if battery is charged. Mains electricity can also be used during stationary periods.	Vans. Small and medium trucks.
	Auxiliary alternator	Similar to vehicle alternator drive, except a separate alternator is used. Fan motors used for air distribution and heat exchangers are also powered from the alternator output.	Vans. Small and medium trucks.
Independent	Auxiliary diesel unit	A separate small diesel engine is coupled to the compressor. Disadvantages of addition weight and emissions, but is used where high level of cooling capacity is required.	Larger vehicles.

Although manufacturers quote the cooling capacity of onboard refrigeration systems at full load, in reality these systems operate at a range of loads to match the refrigeration duty cycle and to maintain cold storage temperatures. As a result, the compressor operates under transient conditions which results in a reduction of efficiency and lifetime of the compressor. To reduce the transient load conditions of the compressor in VC refrigeration systems, these systems can be hybridised with non-mechanical refrigeration systems. Such hybridised systems have been known to reduce the size of the compressor and allow stable operation of the compressor in VC systems [20].

2.1.3.2 Onboard Non-Mechanical Refrigeration Systems

Phase change materials (PCM) and eutectic compositions are used to absorb heat entering the refrigerated space - these materials are usually filled into beams, plates or tubes [12, 20, 29]. The PCM or eutectic material is frozen by connecting the installed system to mains electricity when the vehicle is not being used. Freezing is normally done at night to take advantage of off-peak electricity costs. These systems can work both with and independently of a mechanical refrigeration system and are silent and reliable in operation [12, 20, 29].

Other non-mechanical systems use cryogenic nitrogen or carbon dioxide, which is sprayed into the vehicle [29]. These systems are known as total loss systems as the refrigerant is not recycled as in a VC or sorption systems. While these systems are expensive, particularly when used for long journeys, they are silent in operation and provide rapid pull down temperatures.

2.1.4 Attempts to reduce energy consumption of onboard refrigeration systems

As sorption refrigeration systems use a thermal compressor (Figure 3), the exhausts of ICE engines could, in principle, be used to power these. HGV diesel engines of 225 to 525hp produce 46.3 – 58kW to the cooling system and 39.5 – 141.5kW to the exhaust [30].

Temperatures are particular important when operating sorption refrigeration systems as discussed earlier in this report. From HGV Diesel engines of 225 to 525hp, temperatures from 80 to 100°C are available from the engine coolant loop and 370 to 490°C from the vehicle exhaust [30]. Therefore the heat available from both the coolant loop and exhaust is sufficient to power various sorption based systems

The integration of unutilized exhaust heat and sorption systems has been studied in an attempt to reduce energy consumption of onboard refrigeration. Manzela et al [31], using a domestic refrigerator, tested the feasibility of integrating an ammonia – water absorption refrigeration systems and automotive exhaust. Using a 1600cc, 8 valve petrol engine in the experiment, they confirmed that automotive exhaust gases can potentially power absorption refrigeration systems. However, this system provided a low COP and the cooling capacity of the system was not adequate for transportation applications. The work concluded that, with an appropriate absorption refrigeration system, the cooling capacity produced could be used for automotive cabin air conditioning.

2.1.5 Energy Usage of Onboard Refrigeration Units

Christy and Toossi [30] identified the cooling capacity required in refrigerated transportation. It has been estimated, with a 35°C ambient temperature, that large truck refrigerated trailers and small to medium sized trucks require cooling capacities of 13.5 – 18.8kW and 5.9 – 8.9kW respectively [30]. Hubbard calculates the cooling capacity in all vehicles by using Equation 4 [32].

$$Total\ Load = Trans.Load + Service\ Load + Product\ Load \qquad \text{(Equation 4)}$$

Where:

Trans. Load is the heat leaking though the vehicle body

Service Load is the that enters the vehicle during door openings

Product Load is the heat given off by the products being transported. However in calculating cooling capacity, this value is very small and can be ignored.

Christy and Toossi also identified that an onboard refrigeration unit can consume an additional 10% fuel compared with a non-refrigerated vehicle [30]. Data from Unilever has stated that the additional fuel consumption is much greater and the additional fuel consumption is 24% [33].

To find the fuel consumption, energy consumption and carbon emissions from current onboard refrigeration units, data from Thermoking and Hubbard was reviewed. Figure 6 shows the relationship between the calculated fuel consumption against cooling capacity at -18°C of trailer and truck refrigeration units by Thermoking [8]. Table 11 shows a summary of calculated COP of these units [8]. The data and the methodology of calculating COP is highlighted in the Appendix of this report.

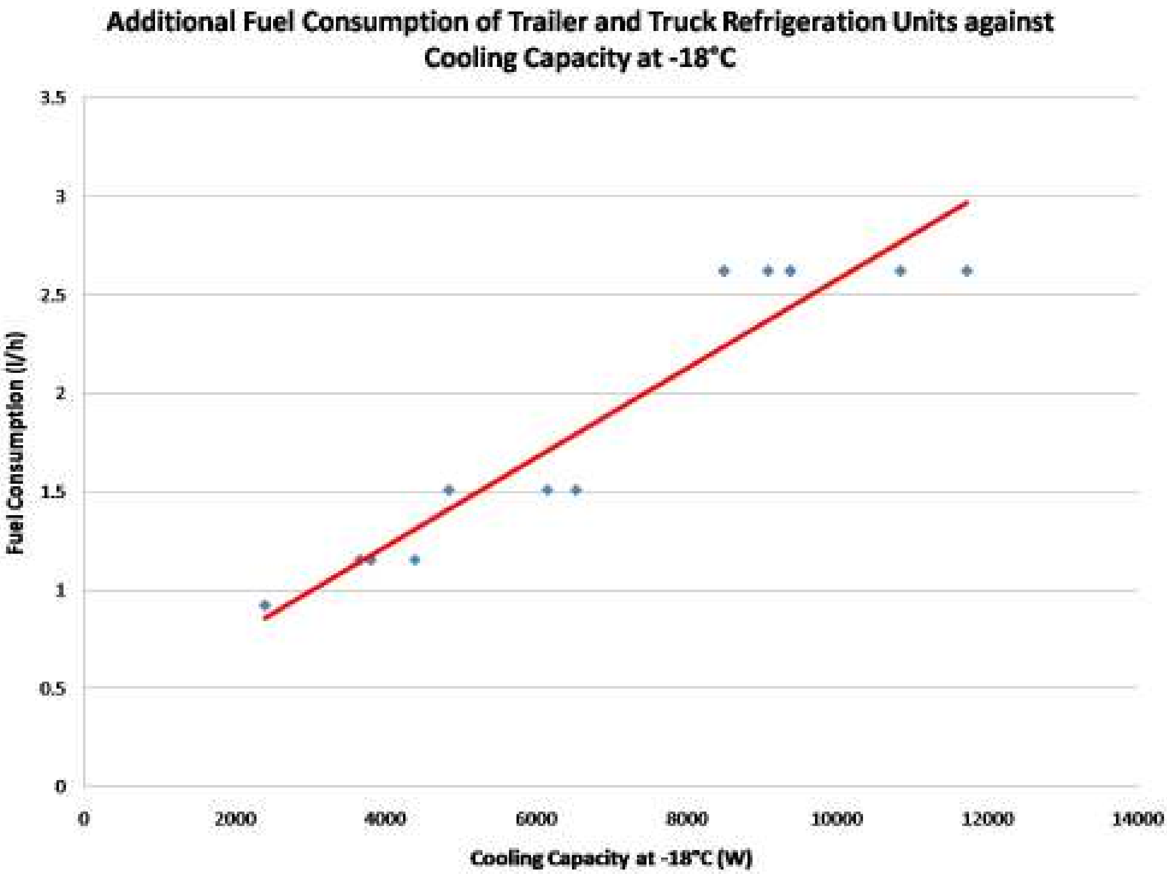

Figure 6 - Variation of Fuel Consumption with Cooling Capacity for Commercial Delivery Vehicles

Table 6 – Summary of commercially available onboard refrigeration units [8]

Refrigeration unit type	Mean COP		Standard deviation		COP at 0°C		COP at -18°C	
	0°C	-18°C	0°C	-18°C	H	L	H	L
Trailer	1.67	1.04	0.20	0.12	1.87	1.48	1.16	0.93
Truck	1.50	0.97	0.29	0.15	1.78	1.21	1.12	0.82

Data for the power requirement for direct drive units is not supplied by refrigeration unit manufacturers. Reviewing the data for independent trailer and truck refrigeration units, it can be calculated that for air temperatures of -18°C, a mean COP of and 1.04 and 0.97 can be observed respectively. Since truck units provide cooling capacities closer to that of direct drive systems, the mean COP value for truck units plus/minus the standard deviation of this data was used. This provided COP values of 1.12 and 0.82 at -18 °C. From these COP values, a reverse calculation was conducted and Figure 7 shows the calculated fuel consumption at different cooling capacities (at -18C) for Hubbard and Thermoking refrigeration units.

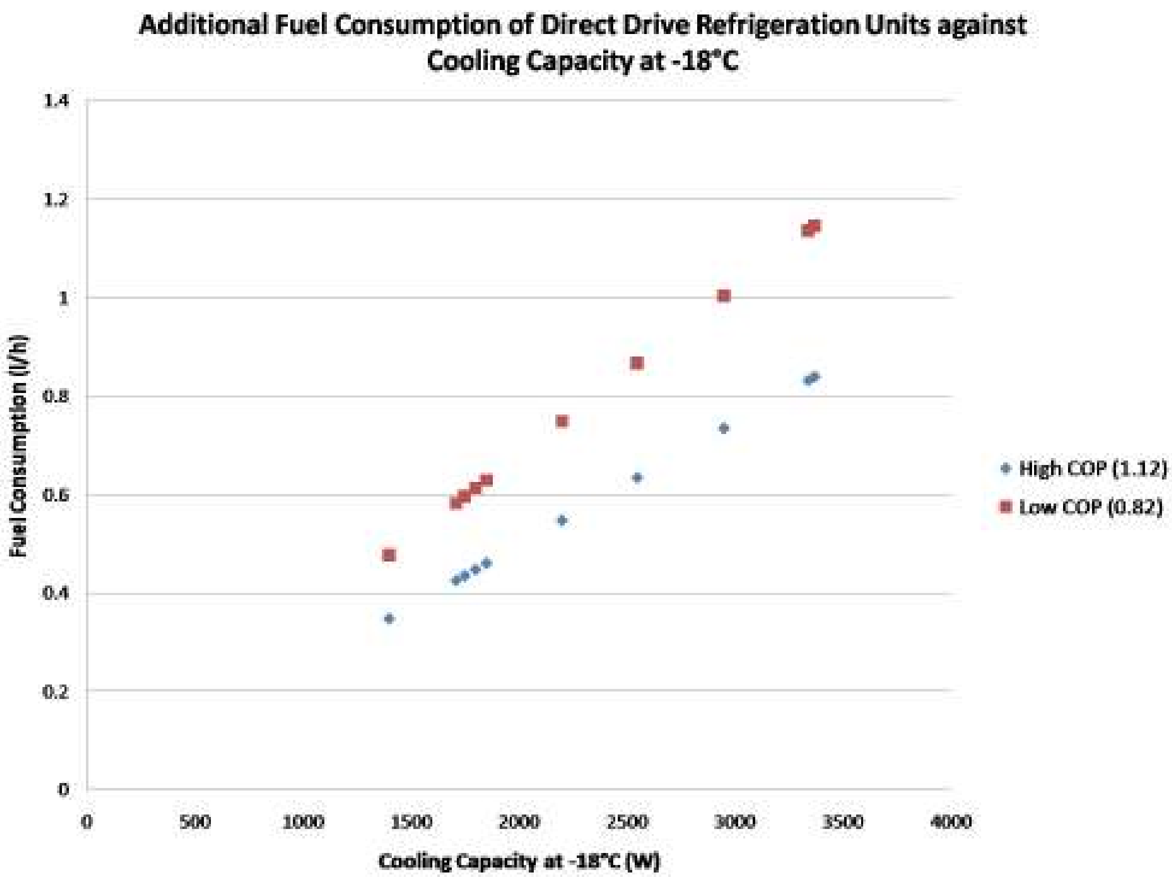

Figure 7 - Additional Fuel Consumption in refrigerated delivery vehicles using direct drive refrigeration systems

From the above data, it can be seen that cooling capacity requirements are dependent on vehicle size and operating conditions. As the cooling capacity requirement increases, fuel consumption increases - this is highlighted in Figure 6 and Figure 7.

From the refrigeration unit data obtained, a trailer with an installed Thermoking SB-400 refrigeration unit will consume an additional 2.62 l/h of diesel compared to a non-refrigerated trailer. Assuming that this type of vehicle travelled at a constant speed of 100km/h during long haulage (60mph national speed limit in the UK on motorways for HGVs greater than 7.5 tonnes [34]), from Table 4 - Calculated Fuel Consumption, Energy Consumption and Carbon Emissions for a Range of Commercial Delivery Vehicles[27, 28]Table 4 we can observe that at full load a refrigerated long haulage vehicle will consume a minimum of 6% more diesel per hour than a non-refrigerated vehicle.

2.2 Hydrogen Fuel Cells

A fuel cell is defined as an electrochemical cell that combines a fuel source with an oxidant (which can be atmospheric oxygen) in the presence of a catalyst to produce an electrical current [35]. The first working fuel cell was demonstrated by Sir William Grove in 1839 by demonstrating the reverse of water electrolysis [36]. Modern hydrogen fuel cells can be fuelled by a diverse range of fuels. In high temperature fuel cells, hydrocarbon fuels such as methane and propane can be internally reformed to produce hydrogen, due to the high temperature and pressures within the cell [36]. However the direct use of hydrocarbons produces carbon emissions at the exhaust of these fuel cell stacks. Using pure hydrogen eliminates direct carbon emissions and only water vapour is released. Complete elimination of carbon emissions would only be possible with the use of hydrogen produced via a non-carbon route. Much research is being undertaken in this area [37-39]

There are many variations of fuel cells which are named after the electrolyte or fuel used. Different fuel cell types have different operating temperatures, pressures and power densities and therefore have different applications. Table 7 summarises these fuel cells and their applications.

Table 7 - Overview of Fuel cells and their Applications [35, 36, 40]

Fuel Cell Type	Mobile Ion	Operating Temperature (°C)	Applications
Direct Methanol (DMFC)	H^+	20 – 90	Portable electronic systems of low power and long running times
Proton Exchange Membrane (PEMFC)	H^+	30 – 100	Vehicles, low power CHP and mobile applications
High Temperature Proton Exchange Membrane (HT-PEMFC)	H^+	130 – 200	Vehicles and low power CHP
Alkaline (AFC)	OH^-	50 – 200	Used in NASA space missions. CHP and in electrolyser applications
Phosphoric Acid (PAFC)	H^+	~220	CHP systems
Molten Carbonate (MCFC)	CO_3^{2-}	~650	Medium to large scale CHP systems up to MW scale
Solid Oxide (SOFC)	O^{2-}	500 – 1000	All size CHP from 2kW to multi-MW

2.2.1 Proton Exchange Membrane Fuel Cell (PEMFC)

PEMFCs have a low operating temperature and high power density as they use a solid state polymer electrolyte membrane made from perfluorosulphonic (PFSA), commercially available as Nafion film [35, 36]. PFSA film forms a Proton Exchange Membrane (PEM), allowing protons to pass from anode to cathode. Also the PTFE backbone of Nafion is hydrophobic. This allows cell to expel water which is produced from the fuel cell reaction [36]. Furthermore the solid state membrane eliminates the use of corrosive aqueous acidic and alkaline electrolytes which require specific handling techniques.

Figure 8 shows the construction of a PEMFC. The Proton Exchange Membrane (PEM) in dark blue is sandwiched between catalyst layers which are applied to Gas Diffusion Layers (GDLs). Finally the whole Membrane Electrode Assembly (MEA) is enclosed in two bipolar plates which allow gas to flow to the MEA and collect current produced from the reaction shown in Equations 5 and 6.

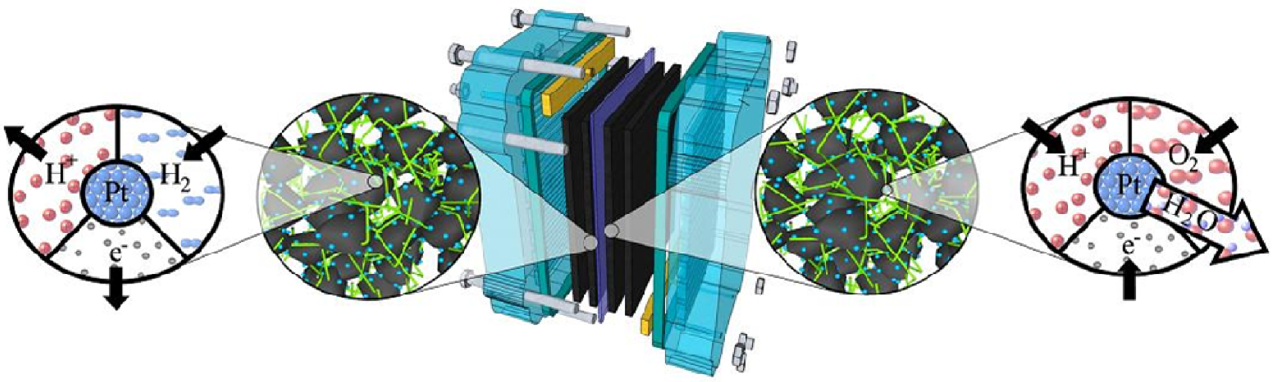

Figure 8 - Schematic of PEMFC and reactions at the electrodes[41]

At the anode, hydrogen is separated into H^+ ions (protons) and electrons in the presence of a platinum catalyst (Equation 5). The positively charged protons pass through the PEM to the cathode whilst the electrons travel through an external circuit to provide a current.

$$2H_2 \rightarrow 4H^+ + 4e^- \qquad \text{(Equation 5)}$$

At the cathode; oxygen, protons and electrons react in the presence of the platinum catalyst to produce water. This reaction at the cathode completes the reaction within a fuel cell and the overall reaction highlighted in Equation 7 is experienced.

$$4H^+ + 4e^- + O_2 \rightarrow 2H_2O \qquad \text{(Equation 6)}$$

$$2H_2 + O_2 \rightarrow 2H_2O \qquad \text{(Equation 7)}$$

PEMFC have many advantages as they have relatively low operating temperatures and quick start up times [36, 42]. As a thin polymer electrolyte layer is used, these fuel cell stacks are small in comparison with other fuel cell technologies and therefore have a high power density compared to other types of fuel cell. Due to these advantages, PEM fuel cells have been used in various automotive and portable applications[43]. In addition these fuel cells have also been used in residential and commercial CHP units[44].

Due to the low operating temperatures of PEMFC, platinum catalyst has to be used to accelerate the otherwise slow reactions at the electrodes. Due to the high price of platinum, these fuel cells are very expensive. However progress has been made to reduce platinum loading resulting in reduced costs. In the 1960s, platinum loading was around 28mg per cm^2 of electrode area [36]; this has reduced to less than 0.2mg per cm^2 in 2009 [36]. Figure 9 shows the breakdown of cost of fuel cells: it can be seen that the total costs are continually reducing due to research in platinum catalyst loading.

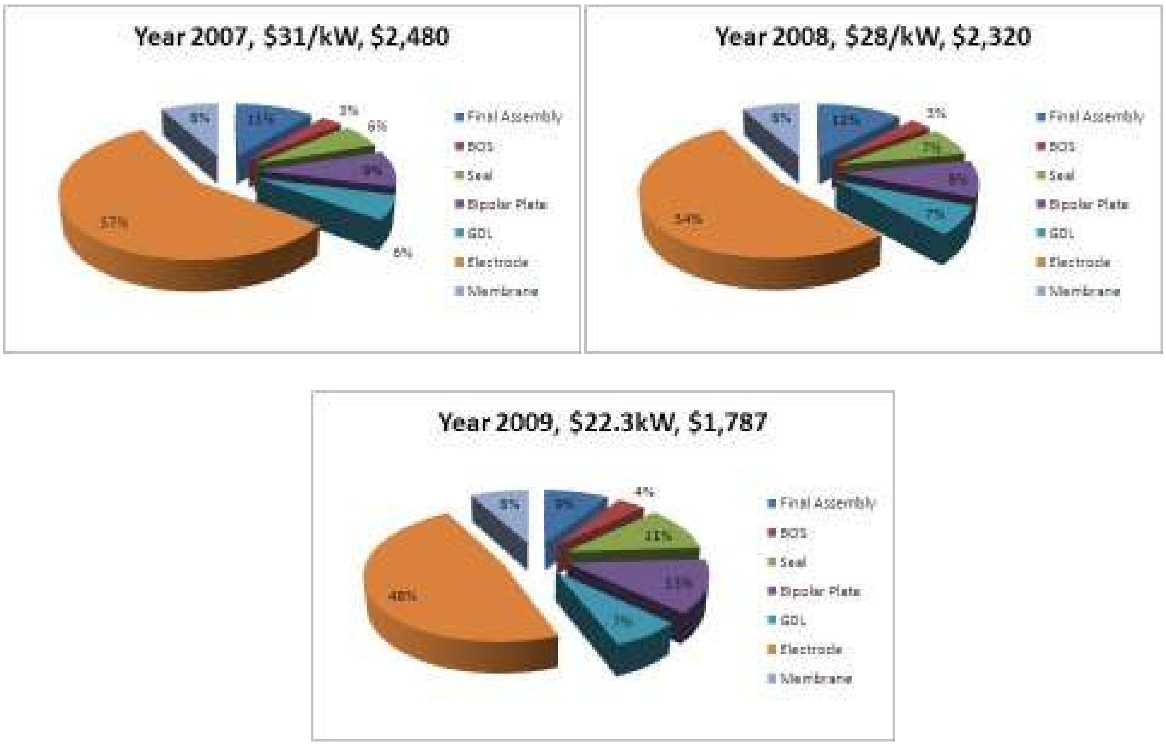

Figure 9 - Cost breakdown of PEMFC production cost per kW of a 80kW mass produced stack (500,000 units) (2007, 2008 and 2009) [45, 46]

Highly pure hydrogen must be used in these fuel cells as the Nafion membranes of these cells are subject to poisoning by carbon monoxide, which is found in hydrogen produced from steam reformed hydrocarbons. Carbon monoxide greatly affects the anode of a PEMFC and even 10ppm can cause an unacceptable effect, thus hydrogen from electrolysis is preferred [36].

High Temperature PEM fuel cells (HT-PEMFC) operate at higher temperatures (130 - 200°C) which can be used for thermal applications [40]. These high temperature fuel cells have a greater tolerance to carbon monoxide and also have a reduced catalyst loading [47] due to the membranes used and the higher operating temperatures. PFSA membranes used in low temperature fuel cells cannot be used in high temperature cells due to their reduced electrochemical stability at higher temperatures; the following electrolyte membranes are incorporated in the PEMFC [40, 48]:

- modified PFSA membranes which increase electrochemical stability of the membrane as higher temperatures;
- sulphonated polyaromatic polymers and composite materials such as polyetheretherketone (PEEK), sulphonated polyetheretherketone (SPEEK), sulphonated polysulphones (SPSF) and polybenzimidazole (PBI);
- acid-base polymer membranes – phosphoric acid doped PBI.

The use of HT-PEMFC in recent years has been very attractive as a future replacement of low temperature PEMFCs, due to the reduced platinum loading and greater tolerance to impurities in the hydrogen fuel. However due to the higher operating temperature, these fuel cells do not benefit from the instant start nature of low temperature PEMFCs and must be heated before running continuously [40]. This may be an issue in passenger vehicles which only conduct short drive cycles, however during long periods of operation (i.e. a refrigeration system or a long haulage truck) such start up times are acceptable.

In general, the use of fuel cells in both refrigeration and transport are very attractive as fuel cells stacks produce both electrical power and heat. Due to the low temperatures produced by PEMFC, cogeneration ability is reduced. Although HT-PEMFCs are currently in their infancy, HT-PEMFCs have greater cogeneration ability and may provide the a low cost alternative to PEMFCs due to reduced platinum catalyst loading [49].

2.3 Fuel Cells in Refrigerated Transport

The potential use of fuel cells in refrigerated transport creates an application with the ability to utilise both the electrical and thermal power produced by fuel cells, thereby providing high overall system efficiency. The Department of Energy (DoE) in the United States has identified this market, by producing a fuel cell hybrid auxiliary power unit (APU) to power a trailer refrigeration unit [50]. Conventionally, a diesel engine is used to drive the compressor in these VC refrigeration systems which are noisy, polluting and increase overall vehicle fuel consumption. Although the project planned to use a SOFC system to take advantage of fuel diversity, a 1.2kW rated Ballard NEXA PEMFC stack was used. This system in a hybrid layout with lithium ion batteries provided high gravimetric and volumetric power densities of 57W/kg and 27W/l respectively. Although the results highlighted by Dwyer et al. [50, 51] are promising, the refrigeration unit still used a small separate diesel engine. The fuel cell hybrid APU replaced the electric backup during standby mode of the trailer unit but no thermal integration of the fuel cell was conducted.

In other APU systems, SOFC have been used to provide high fuel flexibility and to fulfil the high power requirements of trailer refrigeration units but with no thermal integration [52].

2.3.1 Fuel cells and hybridisation in automotive vehicles

Electric vehicles (EVs) including; battery electric vehicles (BEVs), fuel cell vehicles (FCVs) and fuel cell hybrid electric vehicles (FCHEVs) have shown great promise as a replacement for current ICE vehicles [2, 43, 53]. All EVs eliminate hazardous carbon dioxide, nitrous oxides and particulate emissions which are produced by ICE vehicles, ICE hybrid vehicles (ICE HEVs) and ICEs using alternative fuels such as biodiesel and other fuel additives.

In addition, BEVs, FCVs and FCHEVs are quiet during operation, produce no vibration and require less maintenance due to fewer moving parts. Pure battery vehicles have been manufactured for many applications where [2]:

- noise is an issue - mining and indoor vehicles;
- there is a lack of air - lunar and underwater vehicles;
- Vibration is unacceptable - milk floats.

EVs have been produced for the use in personal transportation however with limited success. Vehicles such as the Tesla Electric sports car and the Mitsubishi iMiEV [43] have highlighted the benefits of pure battery EVs for use as light duty personal transport vehicles. Lead-Acid, Nickel – Metal hydride and Lithium-Ion are common battery types used in electric vehicles [2]. Table 8 shows the comparison of these battery technologies against gasoline and pressurised hydrogen [2, 54]. Although Li-ion battery technology is superior compared to other battery technology, gasoline and hydrogen have significantly greater energy density. In addition to energy densities, battery technology has a maximum charge capacity of 70 - 80% to prolong battery life [2, 55]. Therefore the battery energy density shown in Table 8 will be much lower when in a vehicle system.

Table 8 – Comparison of energy storage systems for automotive applications [2, 54]

Comparison of energy storage systems for automotive applications					
	Gasoline	Hydrogen (70MPa pressure vessel)	Lead acid battery	Ni-MH battery	Li-ion battery
Specific energy (Wh kg-1)	11000	1600	35	70	120
Energy density (Wh l-1)	9700	770	70	140	150

Although battery technology has seen great advances, limitations in this technology prevent EV from replacing the wide range of conventional ICE vehicles currently used. In a review by Rittmar von Helmolt et al. [2], battery technology for vehicles has been described as having many shortcomings, such as: range limitation; long charge times; high cost; low capacity and low cycling ability. Chalk et al. [56] highlighted that several challenges remain for battery technology to fully replace current ICE engines including; high cost, operating temperature, calendar life and energy density compared with hydrogen and petroleum.

The issue of cost has been highlighted by Offer et al. [53] who found that, on a system level, hybrid (HEVs and FCHEVs) vehicles are more cost effective than pure battery vehicles. Offer et al. [53] also state that in drive cycles where power requirement was between 5 – 15kWh, pure battery EV would prove to be cost effective. However with applications above this range, like HGV, hybridisation provides lower cost and greater range [53].

Energy density is a key factor to why pure battery vehicles are not cost effective in HGVs. The energy required to provide traction at high loads in HGVs would result in very high weights and large volumes of batteries. In vehicle dynamics, a high sprung mass of a vehicle can hinder performance and increase fuel consumption [57]. From Table 4, it can be seen that a long haulage HGV truck with a total weight of 60 tonnes (including payload) requires 465.6kWh of energy to travel 100km (assuming 37% brake thermal efficiency). The efficiency of an electric motor, controller and additional equipment is around 75 – 84% [35]. For an electric motor assembly efficiency of 75%, approximately 620.8kWh of battery energy would be required to travel 100km at full load. Assuming that Li-ion batteries have 100% usable charge, a battery weight of 5170 kg and volume of 4140 l would be required. Using the same calculation for a small commercial van, a battery weight of 780kg and volume of 620 l would be required. Such high battery weights are unacceptable and in comparison with the unladen vehicle weights, an additional 20 – 30% in weight would be experienced.

Commercial EVs would place an increased demand on the electricity grid as high currents would be required to charge their batteries. Plans have been put in place to upgrade the existing distribution grid in the UK to accept the increase demand and to incorporate greener electricity generation technology to the grid[58].

Batteries for hybrid commercial vehicle applications need to have high cycling ability due to the drive cycles these vehicles undergo. Table 9 shows a comparison of battery requirements in hybrid systems in commercial vehicles (Trucks and Buses) and Light Duty Vehicles (LDVs) [43].

Table 9 – Comparison of lifetimes and cycles during lifetime operation [43]

	Kilometres	Braking cycles	Charge/Discharge Cycles
Light Duty Vehicle	200,000	800,000	10,000
Truck or Bus	592,000	2,400,000	100,000

Advanced lithium ion technology is capable of up to 10,000 charge and discharge cycles before battery life is compromised [43, 59]. Cyclic ability can also be hindered by the effect of deep discharge and, even in advanced batteries, only 70 – 80% of a battery's charge can be used before the effect of deep discharge affects the battery. Therefore battery technology is not suitable for hybrid HGV applications due to the distances travelled during their lifetime. The use of super-capacitors in hybrid HGVs, however, seems very attractive as these have the ability to undergo more than 500,000 charge/discharge cycles and also do not have the issue of deep discharge[43]. This technology requires research and development as this technology has a very poor energy density and high cost compared to advanced battery technology[43].

Fuel cell vehicles have been the research area for many large vehicle manufacturers as these vehicles eliminate the issues of pure battery vehicles. Vehicles such as the Honda FCX Clarity, GM HydroGen3, Suzuki MR Wagon FCV and Chevrolet Sequel are just a few vehicles that have proved the system and cost benefits over Pure BEVs [2, 43]. FCVs and FCHEVs do not have the drawbacks of ICE vehicles and BEVs. Fuel cells do not have a Carnot limitation on efficiency and efficiencies of 60% (Figure 10) can be achieve from using the electrical power and up to 80% can be achieved in thermal integration applications [55]. Fuel cells also have the benefits of batteries such as no noise, no moving parts and no harmful emissions (only water), however FCVs and FCHEVs do not have long charge times. Wipke et al. [60] from the National Renewable Energy Laboratory (NREL) has analysed data from a 8,700 hydrogen refuelling events: from their data the average refuelling rate was 0.79kg/min. Since compressed hydrogen has a specific density of 1600 Wh/kg [2], and assuming a pure FCV has an efficiency of 60%, an approximate refuelling time of 92 minutes would be required to drive a small commercial van for 100km as shown in Table 4.

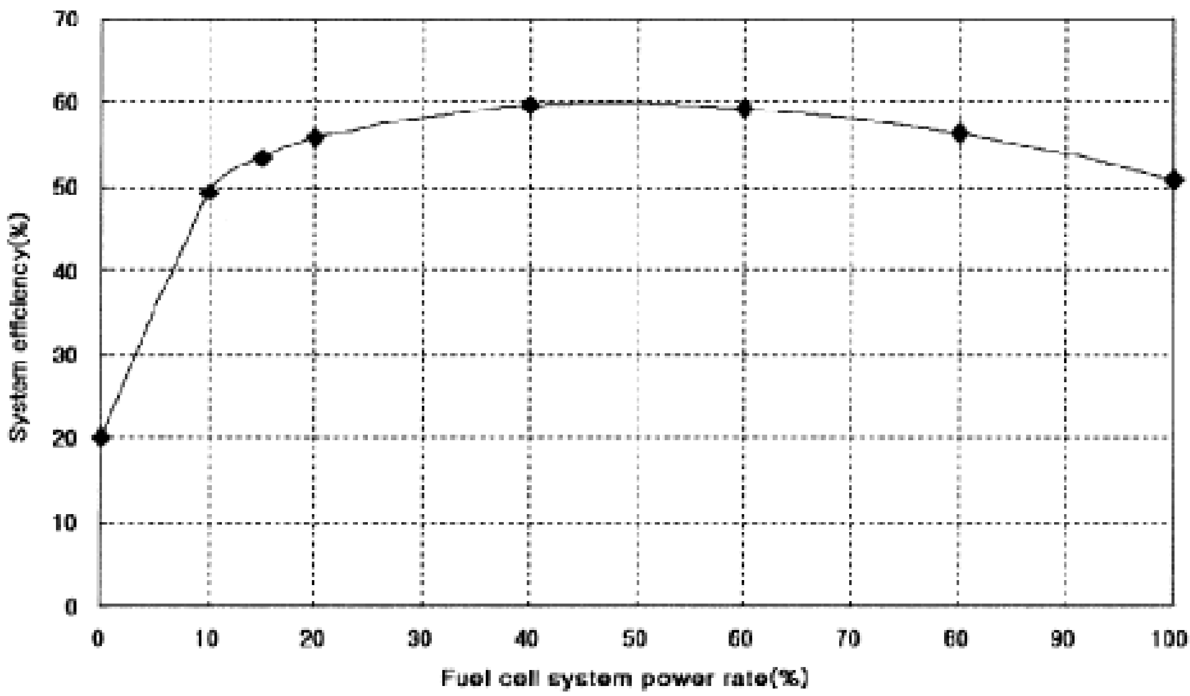

Figure 10 – Efficiency of fuel cell system across power range [55]

FCHEVs have several benefits over pure FCVs [2, 53, 55]:

- Reduced system cost

- Rapid start up of fuel cell system as power to air blowers and other auxiliaries is provided by the battery power supply
- Storage of regenerative braking
- Depending of hybridisation strategy, the fuel cell system can operate at higher efficiencies as the battery operates as a buffer

The key business case benefit to hybridisation is the reduction in system cost. Fuel cells are very expensive compared to battery and ICE technology. Chalk et al. [56] states that the cost of current ICE technology is \$25 – 35 kW-1 and fuel cell systems are five times the cost (\$125 - \$175), even when cost savings of mass production are applied. In research conducted by Jeong et al. [55] fuel cell costs are estimated at \$1200 per kW without mass production savings. Figure 11 shows the reduction of system cost of hybridisation of FCVs. The graph shows that there is a limit in fuel cell cost when hybridisation becomes costly which is approximately \$400 per kW [55]. However this is assuming that battery costs will remain the same.

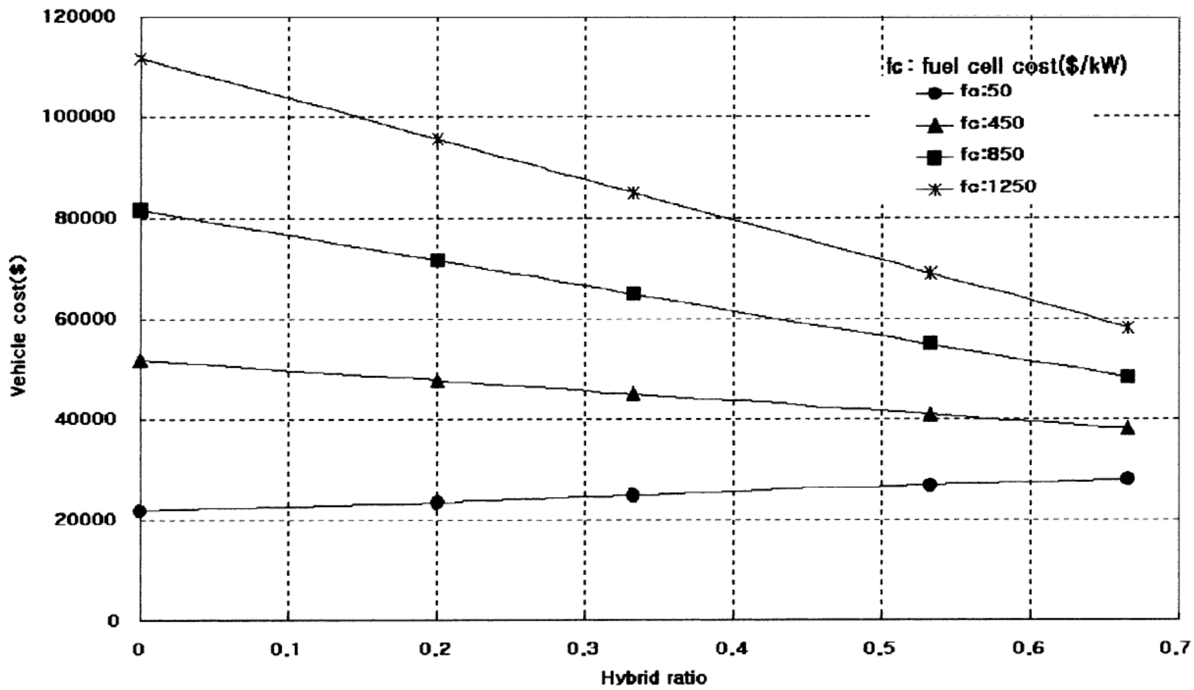

Figure 11 – Cost savings of hybridisation in fuel cell vehicles [55]

Hybridisation strategies are important when calculating the size of fuel cell and battery within a FCHEV system. The most basic hybridisation strategy is when the vehicle only powered by the vehicle battery and the fuel cell system operates as a battery charge (range extender). The fuel cell is switch on and charges the battery when the state of charge (SOC) is below a limit set by the vehicle controller. The fuel cell system will stop charging when the battery is above the SOC set in the vehicle controller software. This allows the fuel cell to operate at part load and therefore peak efficiency.

The second hybridisation strategy is when the fuel cell charges the battery during low SOC and also provides power to the traction motor. When the power request to the motor is less than or equal to the power of the battery, the fuel cell power will be off (unless charging the battery) and all power to the motor will be supplied by the vehicle battery. When the power demand increases above the battery capacity, the fuel cell will provide the additional power required. In such a hybridisation strategy, the level of hybridisation has an effect on overall system efficiency. Ideally in FCHEVs, at low loads the battery should power the traction motor to ensure that the fuel cell operates more efficiently. Therefore from Figure 10, the battery capacity should be less that 40% of the fuel cell capacity and therefore a hybridisation of around 0.2 - 0.25 would be ideal. However, Figure 12 shows the fuel consumption against level of hybridisation. It can be see that a hybridisation ratio of 0.33 is ideal compared with the predicted value [55].

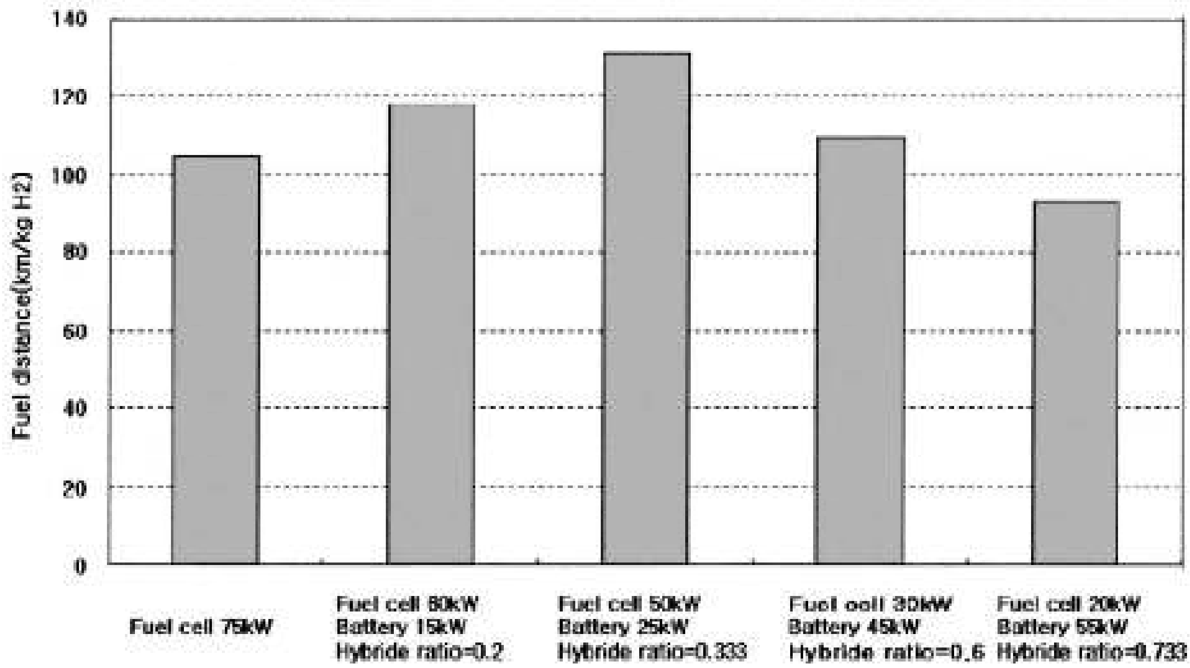

Figure 12 – Comparison of fuel economy for a fuel cell in a hybridised system [55]

Jeong et al. [55] stated that the reason for low fuel economy below hybridisation of less than 0.33 is because the battery is too small to allow efficient operation of the fuel cell system. Also the charge/discharge efficiency is low due to the high battery currents. For hybridisation greater than 0.33, the fuel consumption drops due to the battery power being greater than the fuel cell and therefore the battery becomes the main power source for the traction motor. The charge-discharge time increases due to the battery size and the current from the battery increases providing poor system efficiency.

In summary, FCHEVs are the primary choice as a replacement for current ICE vehicles. These systems have several benefits over ICE vehicles, BEVs and FCVs. A FCHEV would be best to provide greater range [61], relatively low cost and low emissions which is ideal for HGV applications.

2.3.2 Fuel Cells to Power Refrigeration Systems

VC refrigeration systems are often driven by a compressor coupled to an electric motor. Electrical power produced by a fuel cell hybrid system can be used directly to power the electric motor or the electrical power can be stored during low power requirements with the use of a battery or supercapacitor. The fuel cell can also act as a charger, extending the operating range of batteries which provide electrical power for the vehicle's electric motors; Dwyer et al. [50, 51] describe such a system.

Although coupling of an electrical motor to power a refrigeration system is simple, the use of heat generated from fuel cells in Heating, Ventilation and Air Conditioning (HVAC) applications has been a very active topic for research in recent years [62]. Fuel cells can produce both electrical power and heat and in many applications the energy released as heat is unused. In low temperature fuel cells such as PEMFC, this waste heat can equal the electrical power produced, therefore a fuel cell with a rated power of 1kW would produce 1kW as heat [63]. Typical operating temperatures for PEMFC and HT-PEMFC are approximately 30-100°C and 130-200°C respectively [36, 40]. This wasted heat in PEMFC and HT-PEMFC can be used for low heat operations such as low Combined Heat and Power (CHP) and sorption refrigeration systems.

The development of combined heat and power (CHP) and tri-generation systems (combined cooling, heating and power: CCHP) for residential applications have shown great promise for the future. The integration of SOFC and MCFC have been of particular interest as the high operating temperatures of these fuel cells (see Table 7) have the ability to drive sorption refrigeration systems [62, 64, 65]. These systems would also allow the electrical power produced by the fuel cell to be used for other applications. In addition to the high operating temperatures, these fuel cells have high fuel flexibility unlike lower temperature fuel cells [36, 65]. This is highly advantageous as, since a hydrogen infrastructure has not yet been established, fuel flexibility could provide a stepping stone to fuel cell technology for the future.

Fuel cells such as phosphoric acid (PAFCs) and alkaline fuel cells (AFCs) have also been used in CHP applications due to their ability to operate at high temperatures and pressures [36, 66]. These mid temperature fuel cells (~200C) require a separate reformer if operated with alternative fuels, e.g. hydrocarbons, as internal reformation does not occur [36].

High temperature fuel cells require a very high start-up temperature, and therefore require additional heating equipment which adds weight. The high start up temperatures of these fuel cells also results in a slow start, unlike low temperature PEMFC which are preferred in road vehicles [36]. Also, in vehicle applications it is uncommon to have such a high performance heat exchanger onboard to heat these high temperature fuel cells. Typical values for heat exchange are less than 100kW for automotive applications [2]. Phosphoric acid, molten carbonate and alkaline fuel cells use an aqueous electrolyte which may leak due to the harsh environments faced by road delivery vehicles. The results of using a fuel cell with an aqueous electrolyte onboard a vehicle have been highlighted by the GM Electrovan of 1966 where leaking electrolyte was an issue [2].

PEMFC and HT-PEMFC are ideal for automotive applications despite their stringent fuel requirements as these fuel cells eliminate the issues of high temperature fuel cell integration and have greater power density. Therefore PEM fuel cells would be ideal to power both on board refrigeration and traction for a delivery vehicle. However due to the low operation temperatures of PEMFC, the potential to use these fuel cells in cogeneration systems is limited [42]. HT-PEMFC however can provide a solution as the high temperatures produced (130 - 200°C); have the ability to drive various sorption refrigeration systems. Prototype residential PEM fuel cell based CHP systems have been developed [44]. These systems are mainly in the range of a few kW, which is ideal for household power requirements.

Modelling the thermal integration of PEMFC for refrigeration applications has highlighted the possibility of using low grade heat of PEMFC. Pilatosky et al. [63] have modelled an automotive air conditioning system (water – monoethylamine absorption refrigeration system) which utilises waste heat from a PEMFC fuel stack. In particular, modelling has shown that a fuel cell stack operating at a low temperature of 60°C can produce a COP close to 0.57 to produce a temperature of 10°C with a 25°C ambient temperature. Monoethylamine is a suitable refrigerant for air conditioning applications, but, for the distribution of frozen foods an air temperature of below -20ºC is required and therefore an alternative refrigerant is required, e.g. ammonia [12, 15]. Other studies have been conducted by Zhang et al. [67] where the low temperature PEMFC have been modelled to assess the maximum efficiency whilst operating an absorption refrigeration system. The results were encouraging, the electrical power output was even enhanced due to the exhaust gases being passed through a heat exchanger to heat inlet gases in a regenerator [67]. Although very few studies have been conducted on PEM thermal integration and the use of these fuel cells in refrigeration, modelling studies have shown potential, and predictions have been made that commercial PEM fuel cell refrigeration hybrid systems may be made available in the near future[67].

3. Vehicle Onboard Refrigeration Model

This aim of this model is to calculate:

1. The refrigeration duty of any refrigerated vehicle
2. The COP at any ambient and evaporator temperature
3. Compressor power required for a VC refrigeration system using the calculated COP and refrigeration duty
4. Compressor power savings when using a dual stage Sorption-VC refrigeration system
5. The generator heat and the fuel cell power required to drive such sorption systems

3.1 Vehicle Refrigeration Duty

In order to calculate the COP and compressor power of an onboard vapour compression system, a vehicle refrigeration duty (cooling capacity) must be defined. Using Equation 4, it is possible to calculate the refrigeration duty of a vehicle refrigeration system. It is assumed that the product load is negligible and therefore is ignored in this model.

3.1.1 Transmission Load

The transmission load is the total heat that penetrates the vehicle body and insulation despite best efforts. Using Fourier's law [19], it is possible to calculate the transmission through vehicle insulation.

$$Q_{Trans} = \frac{k.A.dT}{x} \qquad \text{(Equation 8)}$$

Where:

Q_{Trans} is the heat entering the cold space

k is the thermal conductivity of the insulation and vehicle body

x is vehicle body and insulation thickness dT is the temperature difference between ambient and the cold space

A is the mean surface area

$$A = \frac{A_i A_o}{2} \qquad \text{(Equation 9)}$$

Where:

A_o is the outer surface area of the insulation

A_i is the inner surface area of the insulation

Tassou et al [20] stated that the most commonly used vehicle insulation consists of expanded foam which is sandwiched between plywood. The plywood sheets are reinforced with polyester, steel or aluminium skin to further reduce heat transfer. The most popular foam is polyurethane which achieves a thermal conductivity of 0.022W/mK for the whole construction [20]. It assumed that this construction of vehicle insulation used. As stated in the literature review, there is a constraint of 100 – 200 mm around the inside of the cold space for air distribution and vehicle insulation. It is therefore assumed that the insulation thickness is 50mm.

Due to the effect of defects in the insulation and edge effect, a safety factor of 50% has been added to the value calculated.

3.1.2 Service Load

Service load is the heat that enters the cold storage due to door openings when the product is loaded or unloaded. Table 10 shows the heat entering the cold storage during various door opening patterns [32].

Table 10 - Basic service load during vehicle door openings [32]

Basic Service Load (W/m^3K)						
Door openings per hours	**Opening Duration (Minutes)**					
	3	**4**	**5**	**6**	**7**	**8**
1	0.61	0.62	0.63	0.64	0.66	0.67
2	1.29	1.34	1.39	1.45	1.51	1.58
3	2.04	2.17	2.31	2.4	2.67	2.89
4	2.89	3.15	3.47	3.86	4.34	
5	3.86	4.34	4.96	5.79		
6	4.96	5.78	6.94			
7	6.23	7.59				
8	7.71	9.92		Impractical to operate in this area		
9	9.46					
10	11.57					

The data in Table 10 is then used to calculate the service load of the vehicle by using Equation 10 [32].

$$Q_{Serv} = V.L.dT \quad \text{(Equation 10)}$$

Where:

V is the volume of the cold storage (m^3)

L is the basic service load from Table 10 (W/m^3K)

dT is the temperature difference between ambient and the cold space (°C or K)

3.1 Vapour Compression Refrigeration

In literature review, the typical COP for truck and trailer refrigeration systems is calculated. For truck refrigeration systems, the mean COP for evaporator temperatures of 0°C and -18°C are 1.50 and 0.97 respectively with an ambient temperature of 38°C.

By calculating the maximum reverse Carnot COP from Equation 11 [19], it can be seen that the actual COP of commercially available VC refrigeration systems is a percentage that of the maximum theoretical COP.

$$COP_{Ref} = \frac{T_1}{T_2 - T_1} \qquad \text{(Equation 11)}$$

Where:

T_1 is the evaporator temperature (K)

T_2 is the ambient temperature (K)

After calculation of the refrigeration duty and the COP, by using Equation 12 [19], the power required by the compressor can be calculated.

$$COP_{Ref} = \frac{Q_{in}}{W_{in}} \qquad \text{(Equation 12)}$$

Where:

Q_{in} is the heat removal at the evaporator

W_{in} is the compressor work input

3.1 Dual Stage Sorption-VC Refrigeration

Figure 13 shows the schematic of a dual stage refrigeration system. It can be seen that the condenser (where heat is rejected) of the VC system is coupled with the evaporator (where heat is removed) of the sorption system. The sorption system in a dual stage system removes heat rejected by the VC condenser and also reduces the temperature. Therefore if using waste heat, this system can reduce the VC compressor power and also improve the VC system COP.

Various sorption refrigeration systems can be used for in a dual stage sorption-VC refrigeration system and therefore the details of the sorption system have not been modelled for design flexibility. It is assumed that the refrigerant used in the sorption refrigeration system is water which is capable of using the operating temperatures of PEMFCs and HT-PEMFC at the generator, however these refrigeration systems are capable of producing temperatures above 0°C and therefore a dual stage refrigeration system is required to produce freezing temperatures to store frozen food.

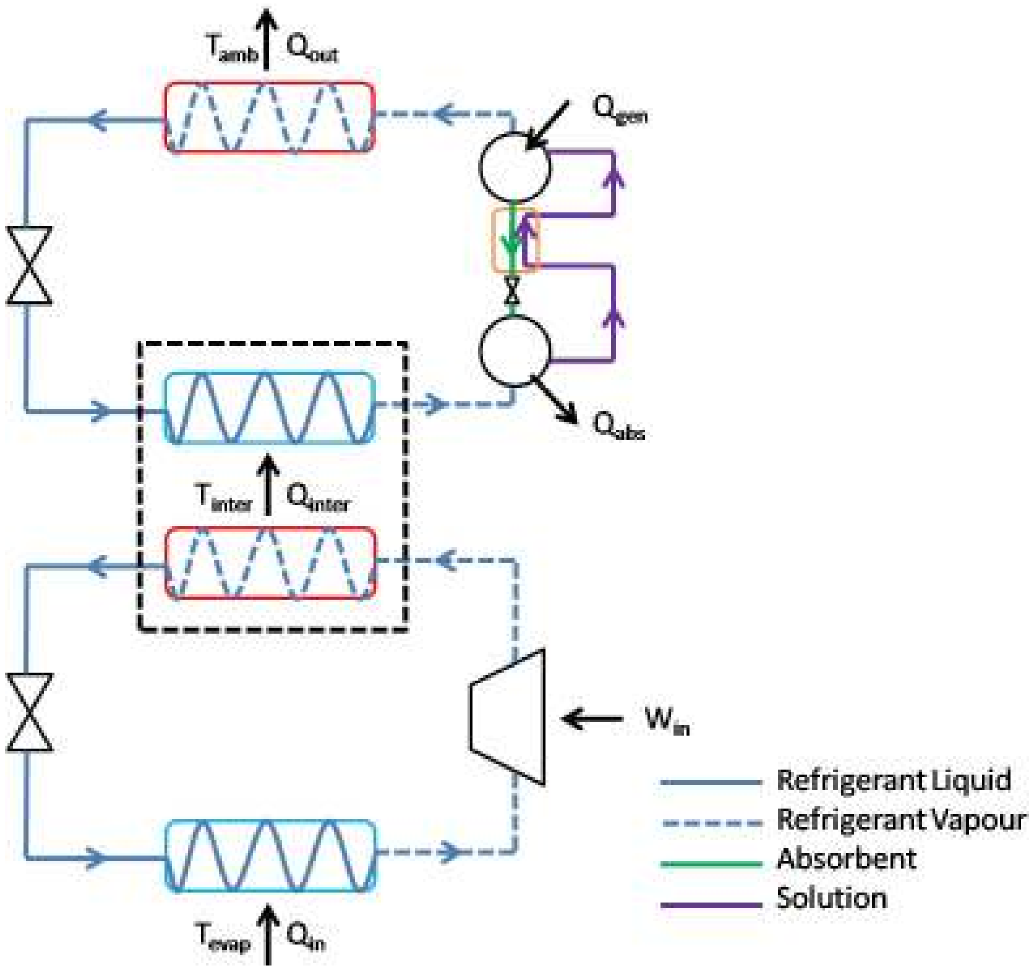

Figure 13 - Schematic of a Dual Stage Sorption-VC Refrigeration System

The COP of the sorption system can be estimated for various ambient and evaporator temperatures in the same way as the VC model. It is assumed that the COP of a sorption system is 0.7 to produce temperatures of 10°C with an ambient temperature of 38°C [14].

The intermediate temperature (T_{inter}) is defined in this model to calculate the heat extraction at the condenser of the VC refrigeration system. To ensure that the sorption system is sized correctly and to ensure that there is no accumulation of heat in the intermediate space, the heat rejected by the VC condenser is the cooling capacity of the sorption refrigeration system. The heat rejected by the condenser is calculated by Equation 13 after the COP of the VC refrigeration system has been calculated [19].

$$Q_{inter} = Q_{in} + W_{in} \qquad \text{(Equation 13)}$$

Once the COP and the cooling capacity has been calculated, like the VC model, the power input can be calculated. For sorption systems, the power input is in the form of heat which can be calculated using Equation 14 [19]. This is assuming that the heat rejection at the absorber is negligible.

$$COP_{ref} = \frac{Q_{in}}{Q_{gen}} \qquad \text{(Equation 14)}$$

Where:

Q_{in} is the heat removal at the evaporator

Q_{gen} is the heat input at the generator

Using the calculated heat input at the generator, it is possible to calculate the fuel cell power by using Equation 15 [36].

$$Q = P_e\left(\frac{1.25}{V_c} - 1\right) \qquad \text{(Equation 15)}$$

Where:

Q is the waste heat produced by the fuel cell

V_C is the cell voltage. It is assumed that the cell voltage is 0.7V which is a typical cell voltage when a fuel cell is operating a maximum power [36].

P_e is the electrical power of the stack

An assumption is made on the individual cell voltage and therefore the calculated fuel cell power is the minimum power required to produce the heat required at the generator.

3.4 Results

3.4.1 Vehicle Refrigeration Duty

The effect of transmission load on vehicle size is investigated in Figure 14. It must be noted that in all delivery vehicles the width is limited to 2.4 to 2.6m [12, 20]. In these results, it is assumed that the vehicle width is constant at 2.5m and the vehicle length is increased at various vehicle heights.

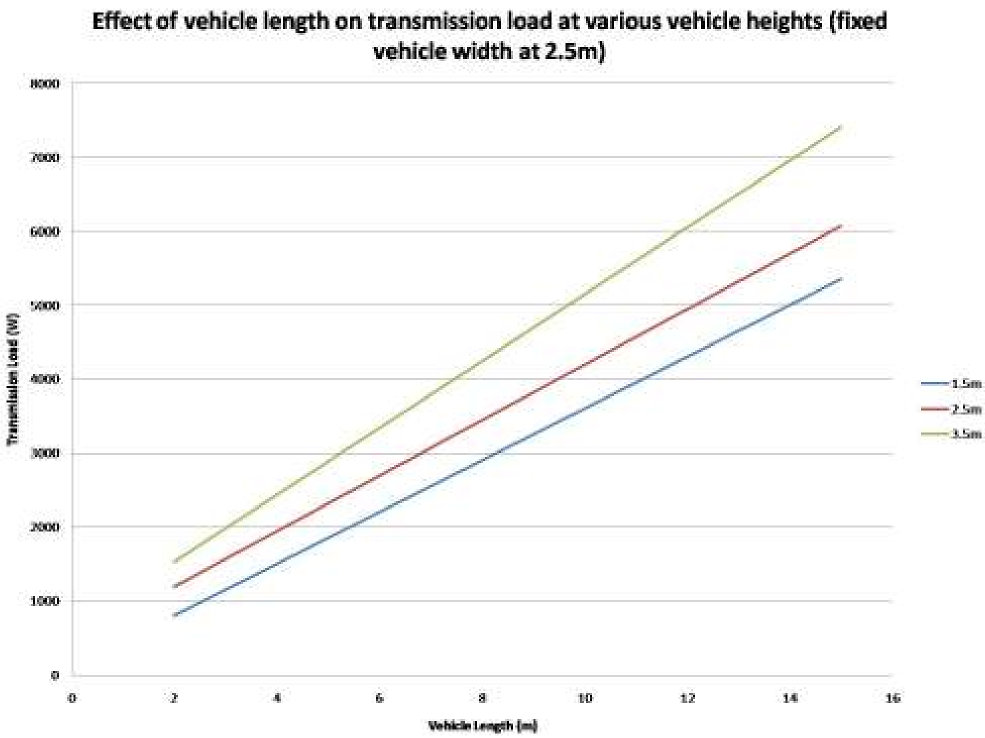

Figure 14 – Effect on vehicle length on transmission load

As vehicle length increases, the average surface area increases proportionally which increases transmission load proportionally. Figure 14 shows this expected trend.

The effect on service load is also investigated using the data from Hubbard [32]. For data representation of the results shown in Figure 17, it was assumed the vehicle has the following dimensions:

- Width: 2.5m
- Height: 2.5m
- Length: 4m

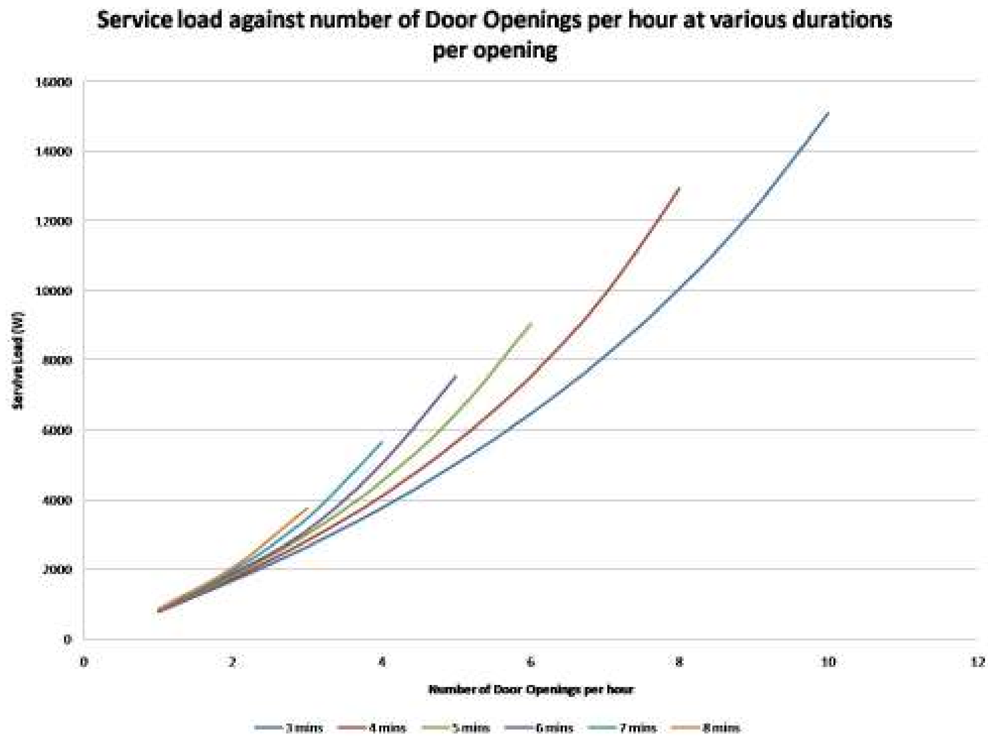

Figure 15 – Effect of door opening frequency and duration on service load

Figure 15 shows the calculated service load at various door opening frequencies and durations. Using Equation 4, the total transmission load and service load provide the cooling capacity of the refrigeration system.

3.4.2 Vapour Compression Refrigeration

Figure 16 compares the COP of commercially available systems and the maximum theoretical Carnot COP. It can be seen that the actual COP of a VC system is 21.3% and 20.9% (evaporator temperatures of 0°C and -18°C respectively) of the maximum Carnot COP.

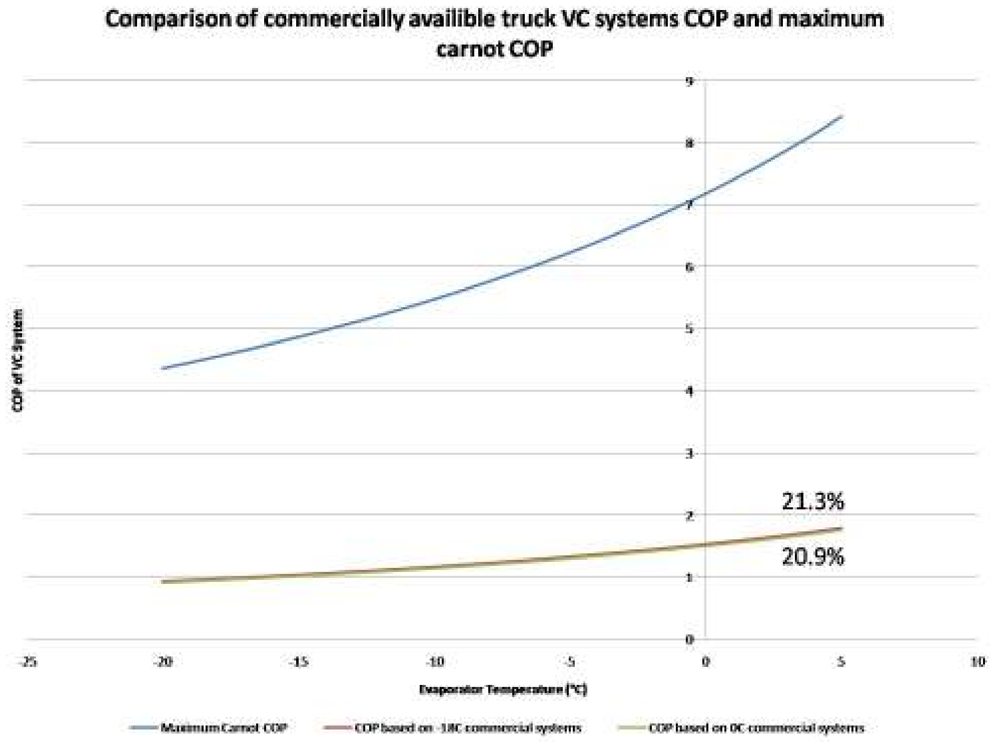

Figure 16 – Relationship between Carnot COP and the COP of commercially available VC systems

Since the actual COP of commercial systems correspond well with the maximum Carnot COP, in remainder of the model it is assumed that the COP at any ambient and evaporator temperature is 21.1% of the maximum theoretical COP.

Using the calculated refrigeration duty and COP, a compressor power is calculated using Equation 12.

3.4.3 Dual Stage Sorption-VC Refrigeration

Using the assumption stated in section 3.1, Figure 17 shows the change in COP and compressor power savings at different intermediate temperatures. It can be seen that the lower the evaporator temperature of the sorption system, the greater the compressor power saving of the VC refrigeration system. This relationship is expressed in Equation 16.

$$Compressor\ Power\ Savings\ (\%) = -0.017(T_{inter}) + 0.655 \qquad \text{(Equation 16)}$$

VC refrigeration system will also operate increasingly efficiently as the COP improves as T_{inter} decreases. The potential cost savings are discussed later is this report.

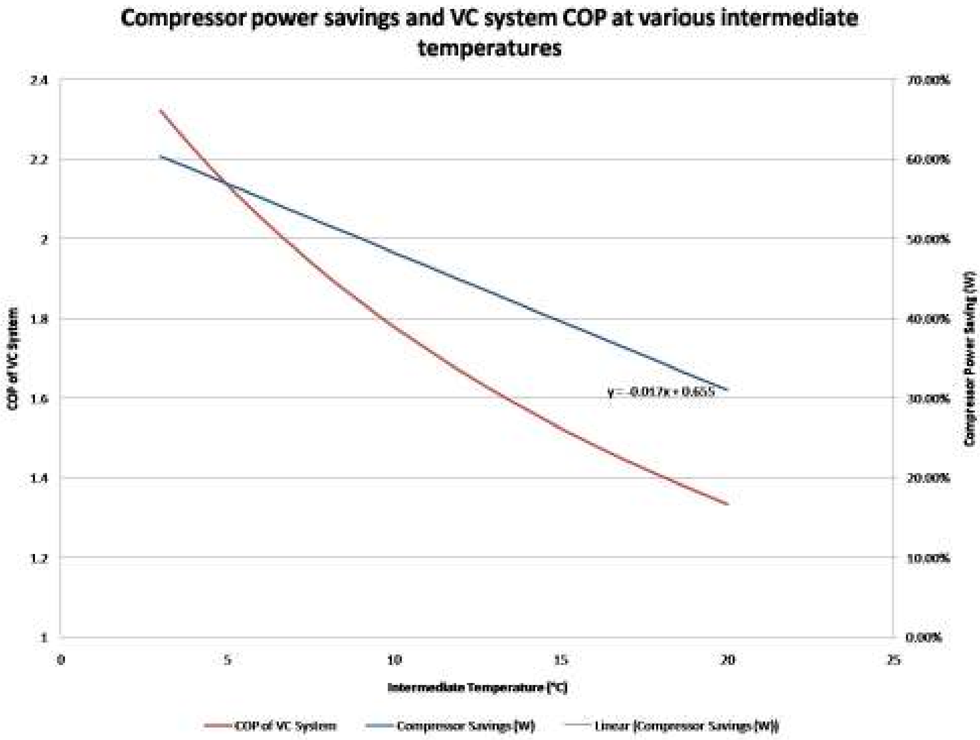

Figure 17 – Compressor power savings and COP of a VC system at various intermediate temperatures

For such dual stage systems to operate the heat at the generator is required and therefore a COP of the system must be defined. This can be estimated by using the same approach as the

VC model. Figure 18 shows the variation in COP against evaporator temperatures with an ambient temperature of 38°C using at the assumptions stated.

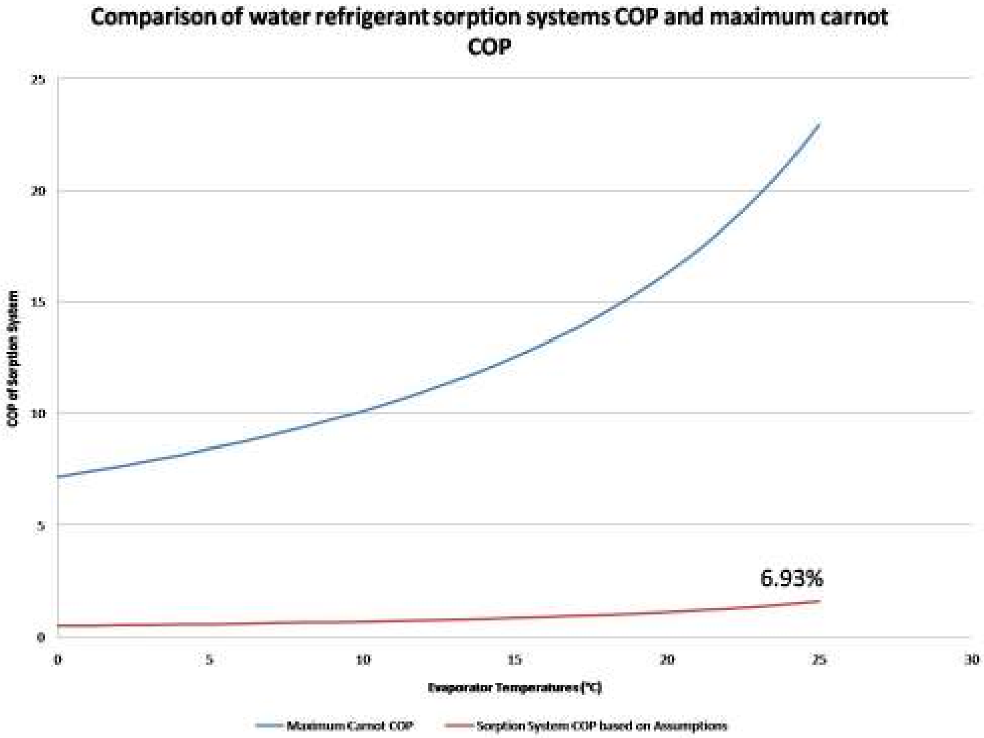

Figure 18 – Relationship between Carnot COP and the COP of sorption systems based on assumptions

From the model data shown in Figure 17, the heat rejected at the VC condenser can be calculated by Equation 13. The heat rejected at the VC condenser defines the cooling requirement of the sorption refrigeration system. Using the calculated COP from Figure 18 and assuming that the heat rejection at the absorber is negligible, it is possible to calculate the heat required at the generator and the minimum electrical fuel cell power required (Figure 19).

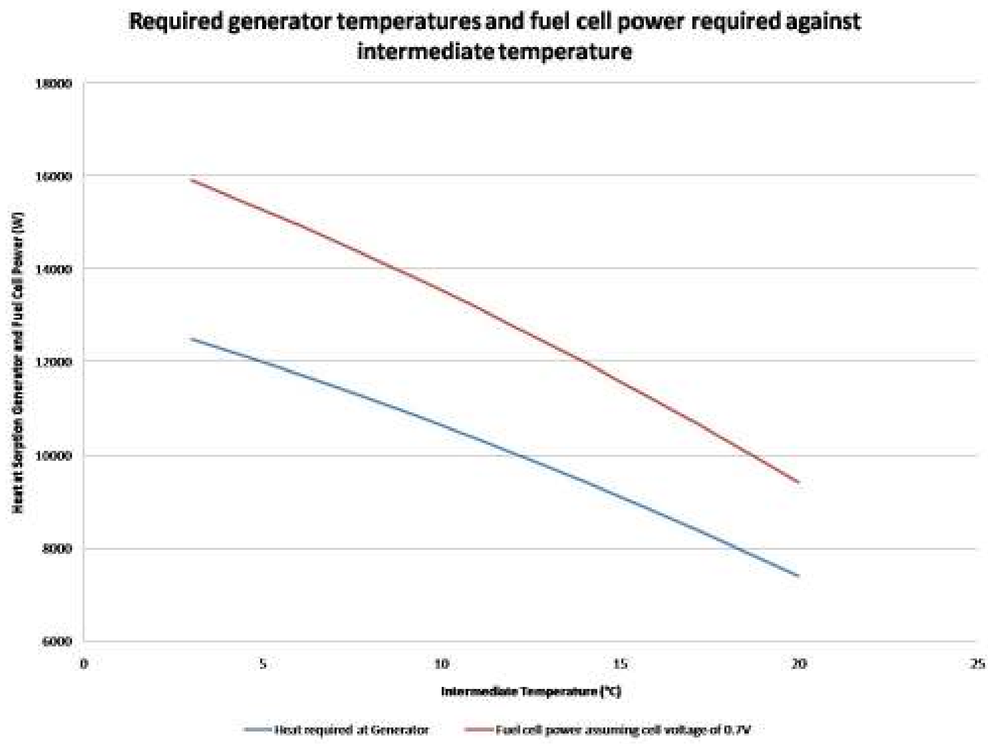

Figure 19 – Required heat at the generator and electrical fuel cell power at various intermediate temperatures (Refrigeration duty of 4769W)

For the sorption system, as evaporator temperature decreases, the heat required at the generator increases. It was observed that the minimum fuel cell power required is an additional 21.4% of the generator heat for any T_{inter} and cooling capacity.

4. Vehicle Model

This aim of this model is to:

- Calculate the power demand of HGVs operating the New European Drive Cycle (NEDC)
- Analyse hybridisation in HGVs to obtain fuel cell and battery power
- Energy consumption of battery and fuel cell of a vehicle during the NEDC

4.1 Power Demand during NEDC

The NEDC is a drive cycle that simulates typical driving conditions in Europe. The NEDC consists of two parts (Figure 20) [68]:

1. Urban drive cycle (four ECE-15 drive cycles)
2. Extra urban drive cycle (EUDC)

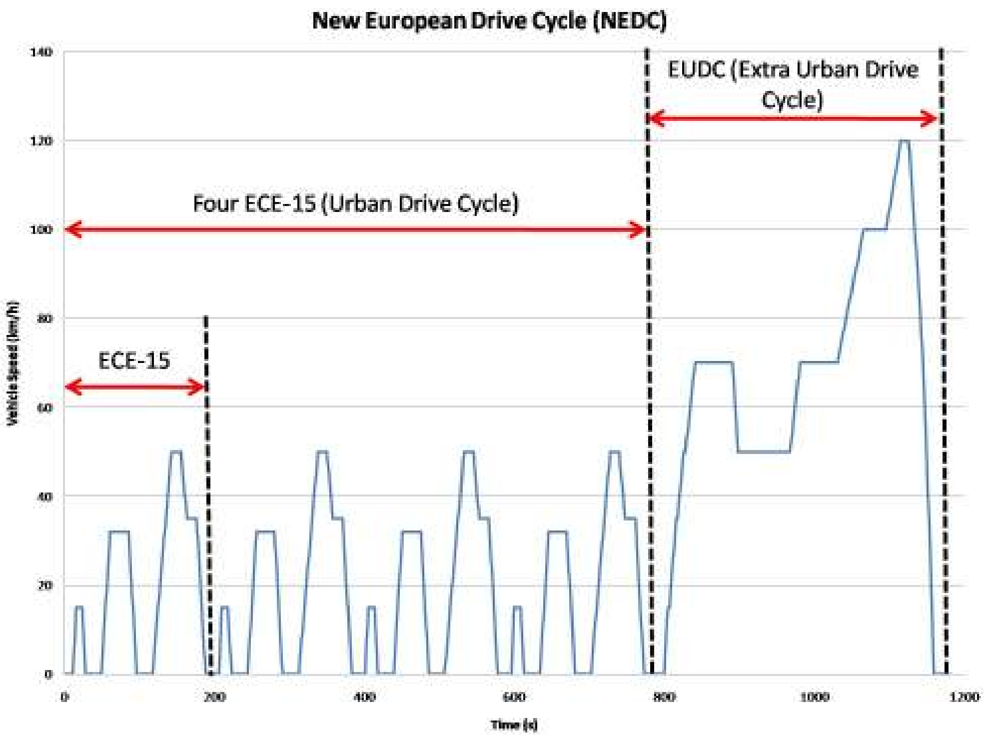

Figure 20 – New European Drive Cycle (NEDC)

To calculate the power demand, the force the vehicle is subject to must be calculated by Equation 17.

$$F_{Total} = F_A + F_D + F_R \qquad \text{(Equation 17)}$$

Where:

F_A is the force required to accelerate to the required speed

$$F_A = ma \qquad \text{(Equation 18)}$$

Where:

m is vehicle mass

a is vehicle acceleration

F_D is the drag force the vehicle is subject to [69]:

$$F_D = \frac{C_D \rho v^2 A}{2} \qquad \text{(Equation 19)}$$

Where:

C_D is the drag coefficient

v is the vehicle velocity

A is the frontal area

ρ is the density of air

F_R is the vehicle rolling resistance [57]:

$$F_R = F_N \mu_R \qquad \text{(Equation 20)}$$

Where:

F_N is the vertical force the tyres are subject to

μ_R is the rolling friction coefficient is a function of speed [57]:

$$\mu_R = \mu_0 + \mu_1 v^2 \qquad \text{(Equation 21)}$$

Where for passenger vehicles [57]:

μ_0 is 0.015

μ_1 is 7×10^{-6} s^2/m^2

From the power demand during the NEDC, it is possible to calculate the maximum energy that can be recovered from braking and therefore this model will also highlight the benefits of a hybridised vehicle.

4.2 Primary and battery power and energy consumption during NEDC

Jeong et al. [55] states that fuel cell hybrid control strategy is based on the battery state of charge. The battery is usually charged when the state of charge is between 20-80% [55]. The power to the motor is provided by both the fuel cell and the battery when operation on the NEDC. When the power to the motor is less than the power to the battery, the battery provides all the motive power and the fuel cell is off. When the power demand is greater than the power of the battery and is less than the fuel cell power, no power is drawn from the battery and the fuel cell provides all power to the motor. During power demands greater than the power of the fuel cell, the additional power is provided by the vehicle battery. The power of to the fuel cell and battery are therefore determined by the level of hybridisation. Equation 22 and 23 show the calculation of battery and fuel cell power based on the Hybridisation factor (H) [43, 55].

$$P_{Battery} = P_{Total}H \qquad \text{(Equation 22)}$$

$$P_{FC} = P_{Total}(1 - H) \qquad \text{(Equation 23)}$$

Where:

P_{Total} is the total maximum vehicle power based on the NEDC

$P_{Battery}$ is the battery power required based on the NEDC

P_{FC} is the fuel cell power required based on the NEDC

H is the hybridisation factor

4.3 Primary and battery energy consumption

The energy consumption of the battery and fuel cell is calculated by Equation 24.

$$E = Pt \qquad \text{(Equation 24)}$$

Where:

E is the energy consumed during time step (Wh or kWh)

P is the power demand during the time step (W or kW)

t is the time step in hours

4.4 Results

4.4.1 Power demand during NEDC

The power requirement of any vehicle during the NEDC can be calculated from the model.

Figure 21 shows an example of the vehicle power requirement during the NEDC.

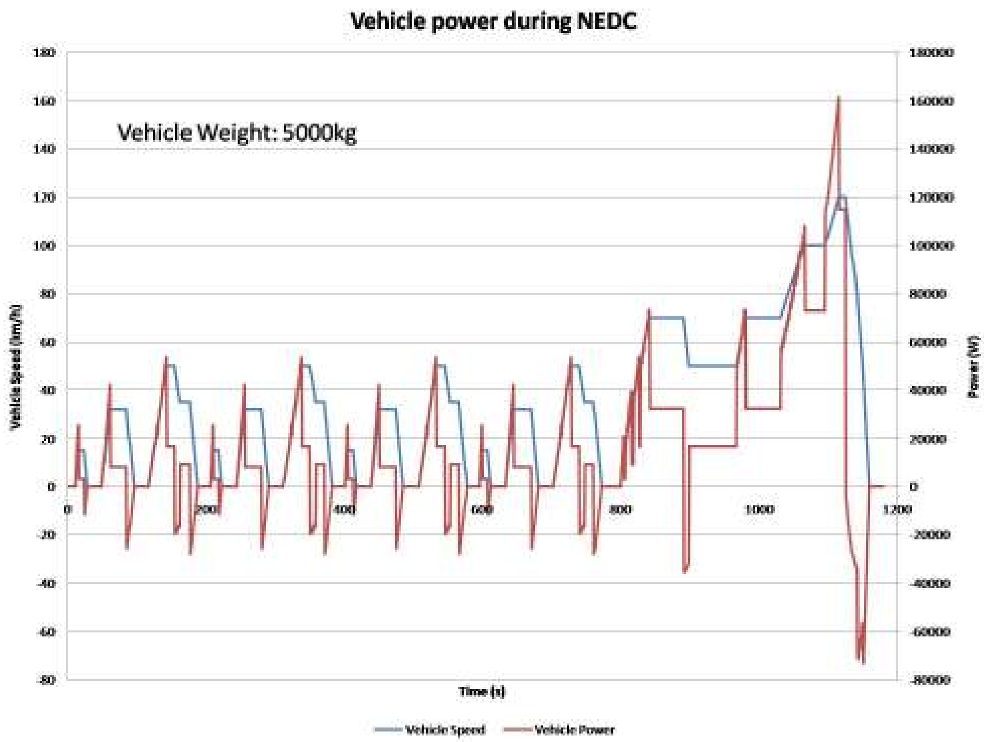

Figure 21 – Example of vehicle power during the NEDC

It can be seen that the negative power requirement can be used for regenerative braking to charge a vehicle battery which is only present in a hybridised vehicle. The lost energy at various vehicle weights and frontal areas can be seen in Figure 22.

It can be seen that there is a maximum energy lost during braking is approximately 30% of the total energy used for traction during the NEDC. The graph also shows that the greater the front area of the vehicle, the lower the energy savings through regenerative braking. This is because energy is lost through drag and therefore cannot be recovered at the brakes.

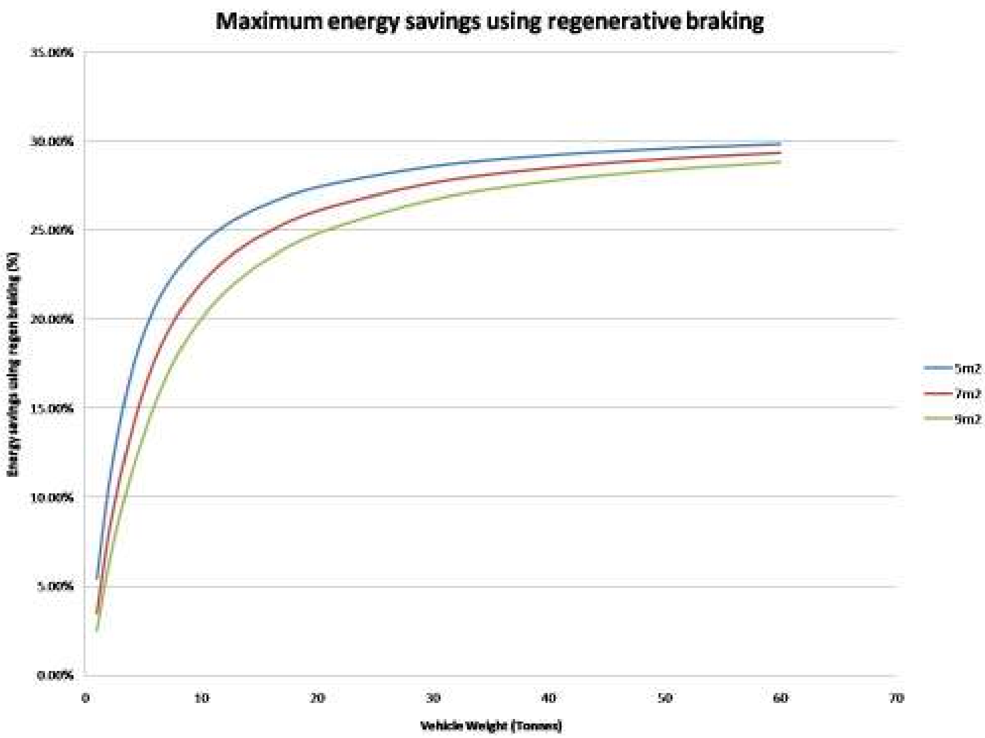

Figure 22 – Energy lost due to vehicle braking

4.4.2 Analysis of hybridisation in HGVs

Assuming a regenerative braking efficiency of 50% [43], a vehicle frontal area of $7m^2$ and also using a hybridisation of 0.33 as stated in the literature review as being the most efficient hybridisation factor, Figure 23, 24 and 25 all show the battery and fuel cell power of vehicles at different weights. It can be seen in Figure 23, that during the ECE-15 urban drive cycle the fuel cell remains off and the battery is providing all vehicle power. The fuel cell only comes on during the EUDC extra urban cycle when the vehicle speed requirement is greater than 50km/h. In this hybridisation, the power set point is greater the 50% of the fuel cell resulting in high efficiencies and the fuel cell is operating for long periods of time which allows the air blower and other ancillaries to respond.

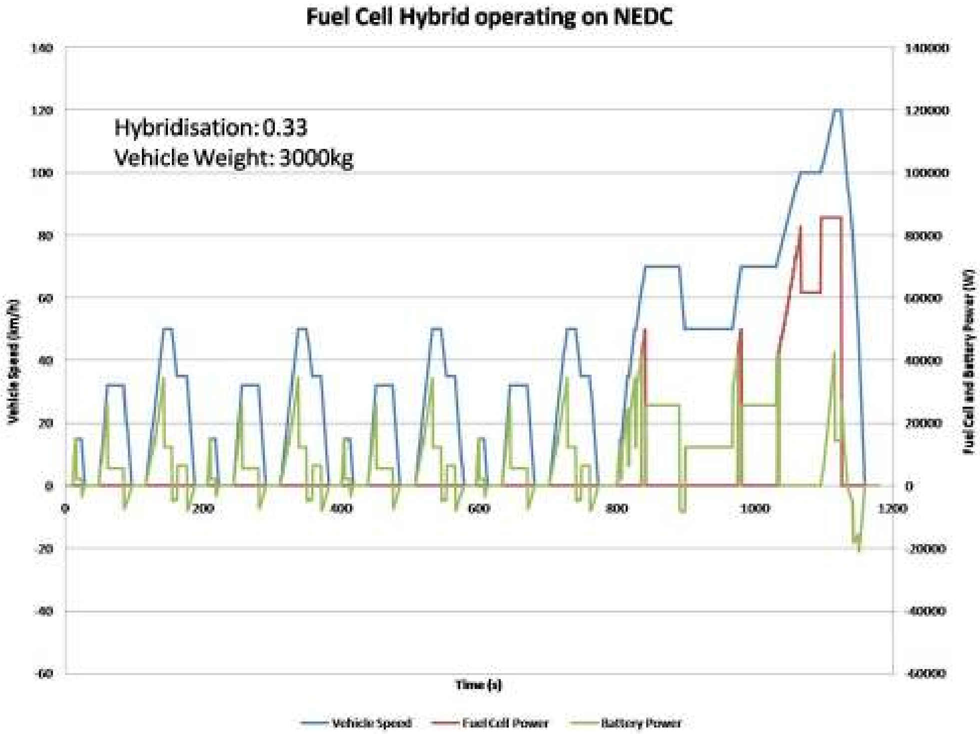

Figure 23 – 3000kg fuel cell hybrid during the NEDC

Figure 24 and 25 shows the same hybridisation of 0.33 however the vehicle weight has increased. In these graphs the fuel cell comes on during the ECE-15 urban drive cycle for very short periods of time. This may be inefficient as it takes time for the air blower and other ancillaries to respond. In addition the fuel cell is operation from zero to 50% power in transient conditions potentially reducing fuel efficiency of the system.

Further investigation is required to investigate the effects of vehicle weight and hybridisation strategy to achieve efficient operation of the fuel cell hybrid system which is discussed later in this report.

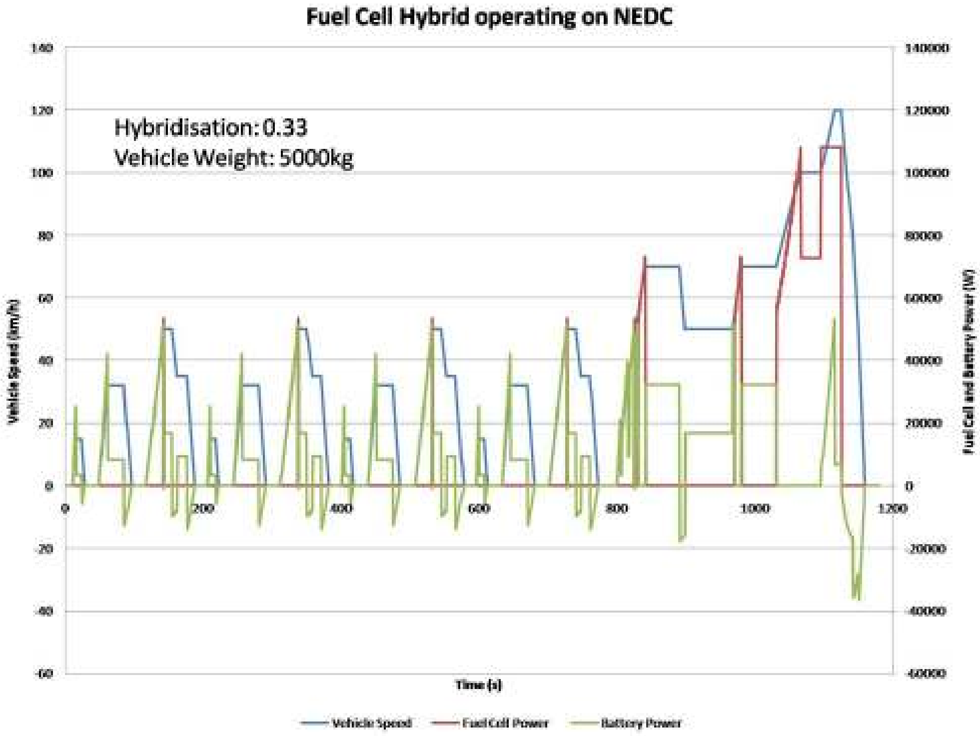

Figure 24 – 5000kg fuel cell hybrid during the NEDC

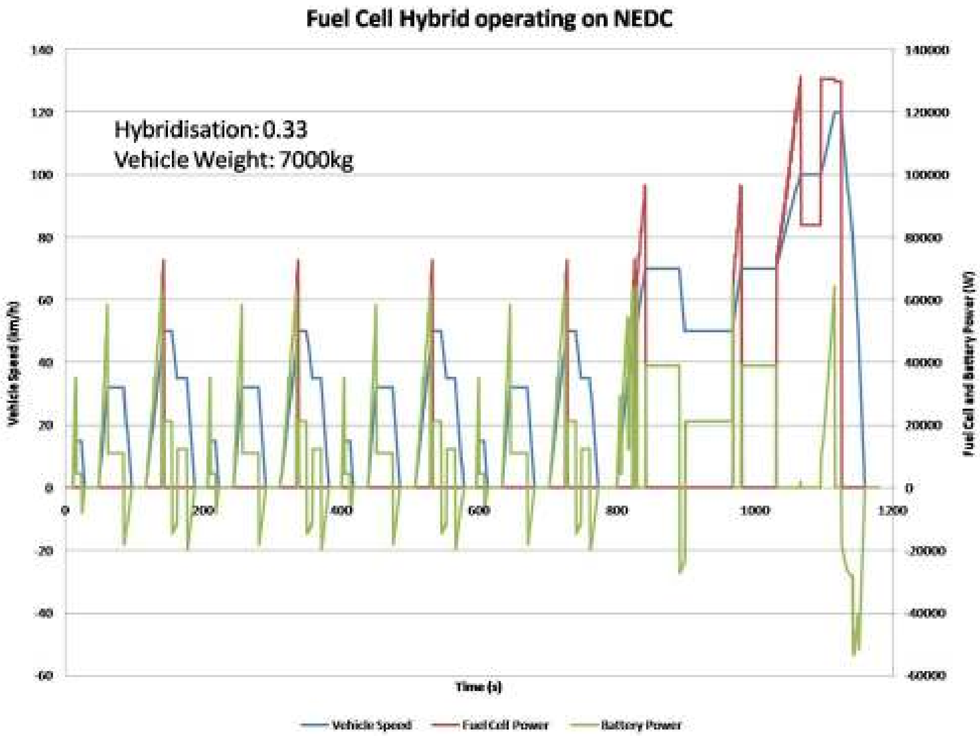

Figure 25 – 7000kg fuel cell hybrid during the NEDC

4.4.3. Energy consumption analysis of battery and fuel cell during NEDC

The energy consumption during the NEDC of the battery and the fuel cell is investigated in Figure 26, 27 and 28. Firstly, as expected, it can be seen that the overall energy consumption increases with vehicle weight.

From the graphs, it can also be seen that as vehicle weight increases at the same level of hybridisation, the fuel cell becomes the primary energy source. For example, at a hybridisation of 0.33, as vehicle weight increases, the fuel cell energy consumption increases and exceeds that of the battery energy resulting in the fuel cell becoming the primary energy source. Figure 28 shows that for greater vehicle weight, the hybridisation point increases when fuel cell energy equals battery energy consumption.

In Figure 26 and 27, it can also be seen that at hybridisation of 0.1, the vehicle battery is only being charged for heavier vehicles, this results in greater energy consumption of the fuel cell at a hybridisation of 0.1. There is also very little change in energy consumption of both the battery and fuel cell above hybridisations of 0.7. However, operating in this region has shown to be very inefficient in several studies vehicle drive cycles above 15kWh [53].

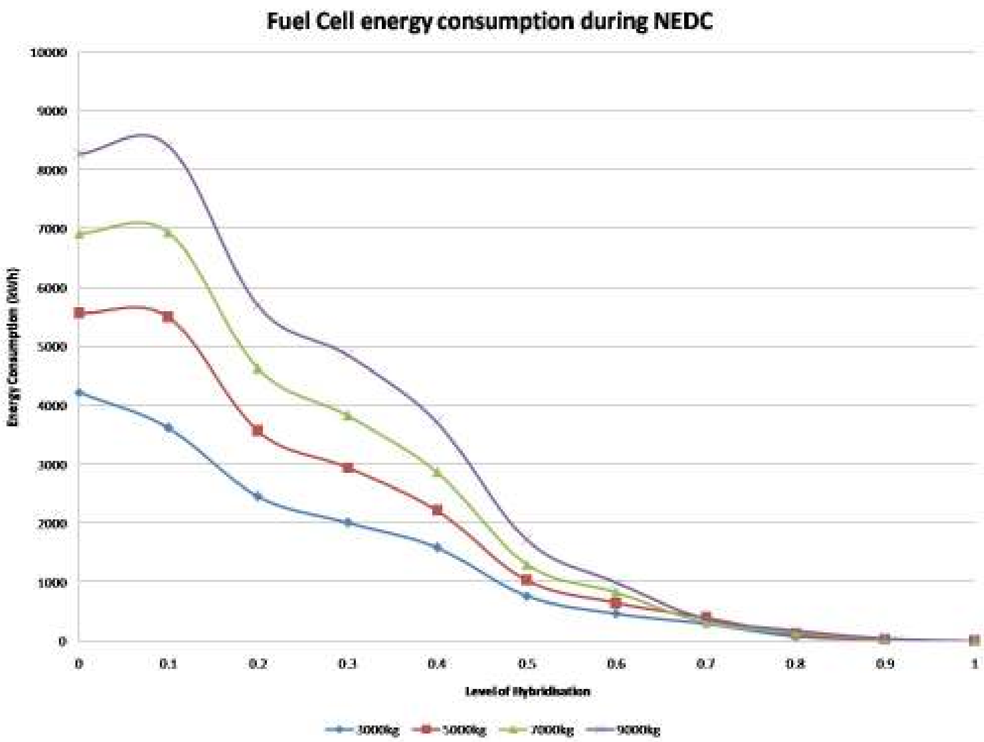

Figure 26 – Fuel cell energy consumption of various vehicle weights and hybridisations

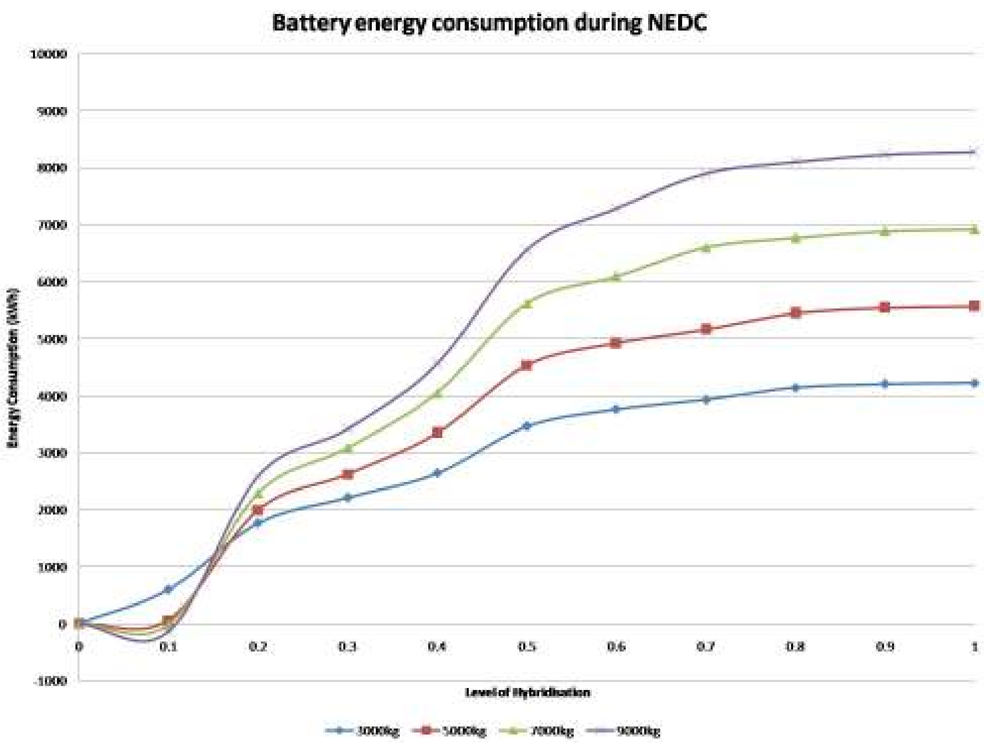

Figure 27 – Battery energy consumption of various vehicle weights and hybridisations

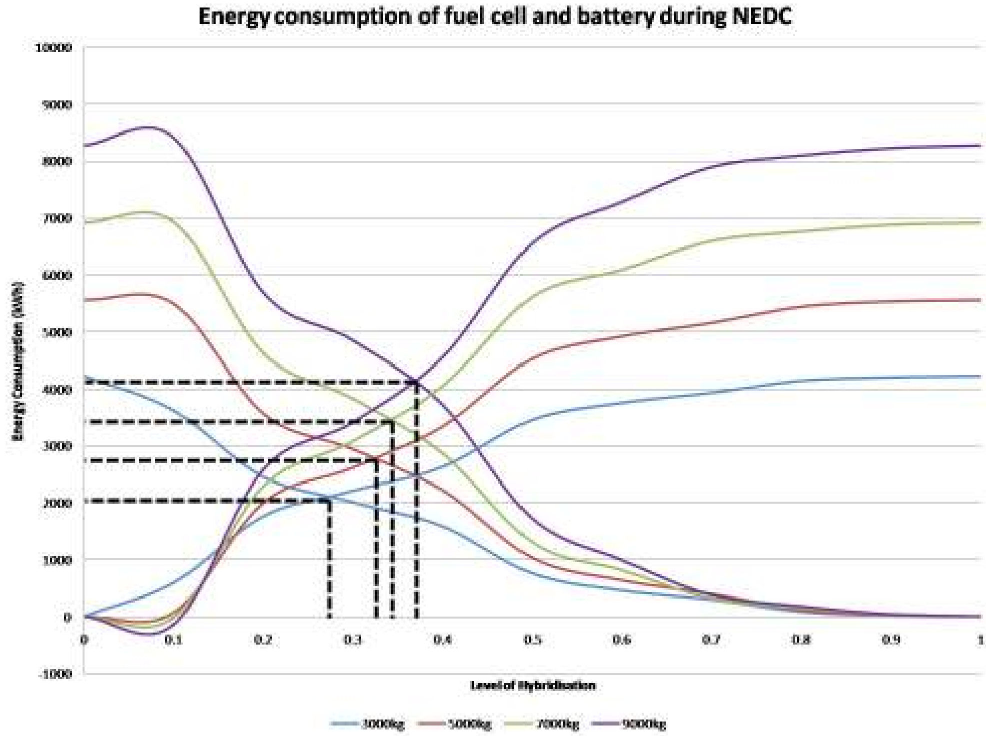

Figure 28 – Energy consumption of fuel cell and battery during NEDC. When vehicle weight increases, the hybridisation point at where fuel cell energy equals battery energy consumption increases.

5. Cost modelling

Before considering the use of a hybrid fuel cell system into a refrigerated vehicle, the associated costs must be analysed to present a business case. The model will calculate the following:

1. Cost of traction during the NEDC
2. Cost of refrigeration per hour of operation at full load

The input energy required from the fuel is calculated

$$E_{input} = \frac{E_{Output}}{\eta} \quad \text{(Equation 25)}$$

Once the input energy is calculated the following fuel energy densities are used:

- Diesel – 9.7 kWh/l [27]
- Hydrogen – 33.3 kWh/kg [70]

The following assumptions were made for efficiencies:

- Diesel engine - thermal efficiency is 37% and the combustion efficiency is 98% [22, 26]
- Fuel cell – thermal efficiency 50%, fuel conversion efficiency 95% and electric motor efficiency of 75% [35, 36]
- Battery – electric motor efficiency 75% [35]

The estimated costs from the literature were found to be:

- Diesel – £1.40 per litre [71]

- Hydrogen – £5.16 and £1.29 per kg for electrolysis and reformation respectively [53]
- Electricity – £0.14 per kWh and £0.05 per kWh for day charge and Economy 7 (night charge) respectively [72, 73]

During cost modelling, it is assumed that the vehicle has the following characteristics:

- Mass of vehicle – 5000kg
- Drag coefficient – 0.5
- Frontal area – $7m^2$
- Cold storage volume – 2.5m x 2.5m x 4m
- Temperature – ambient at 38°C and evaporator at-20°C
- Service – 3 door openings at 4 minutes each opening

When modelling a hybrid vehicle it is assumed that the hybridisation factor is 0.33.

5.1 Results

From Figure 29, it can be seen that the running cost of a pure fuel cell vehicle is the highest and this exceeds the running cost when using diesel fuel, however it must be noted that a pure fuel cell vehicle would be exempt from UK road tax as these vehicles produce zero carbon emissions.

BEVs have the cheapest running costs, however to these vehicles are subject to several shortcomings and also large battery weights would be required resulting a greater fuel consumption cost and reduced vehicle performance [57]. FCHEVs however eliminate these issues and show potential to be a replacement for current diesel HGVs. Although high purity hydrogen from electrolysis is expensive, the use of purified reformed hydrogen has running costs similar to that of battery technology. In addition, research is being conducted to find green and cheaper methods of hydrogen production [37-39].

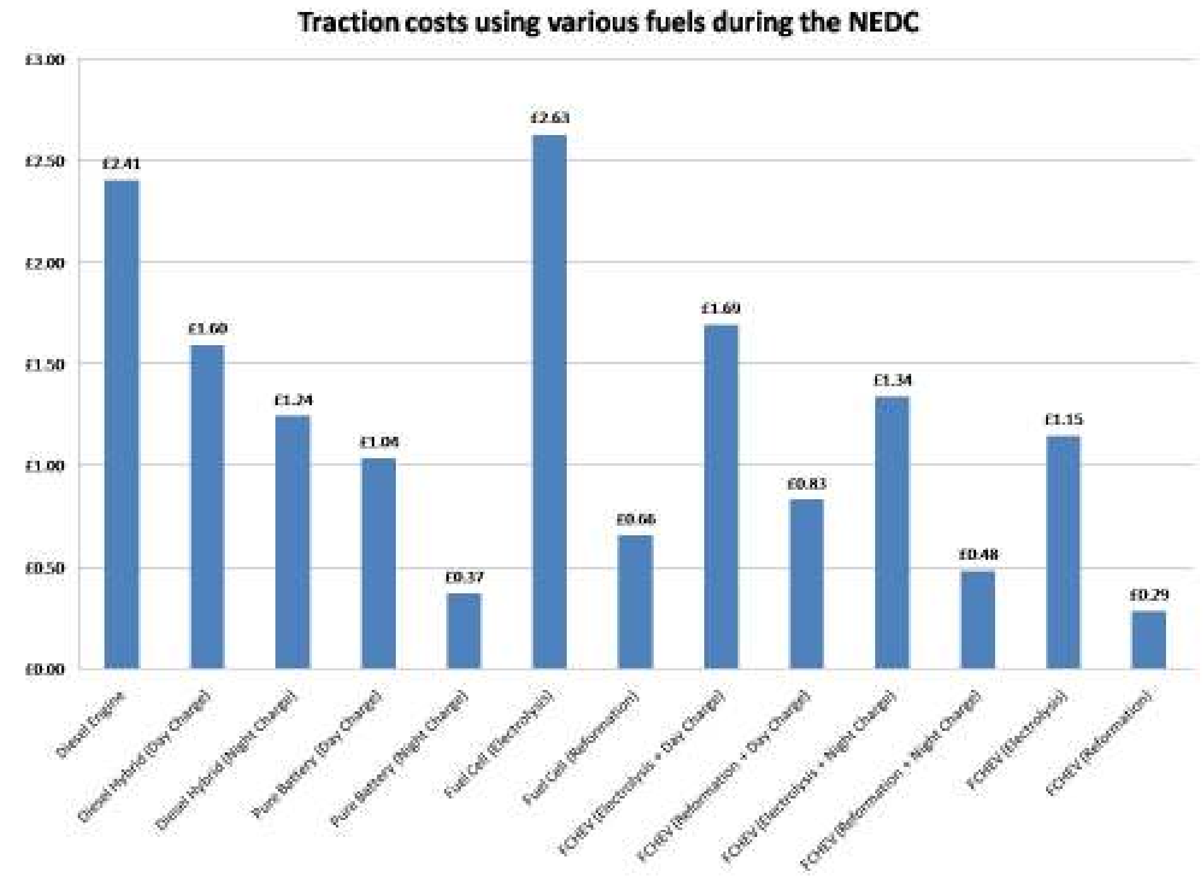

Figure 29 – Traction costs using various fuels during the NEDC

The cost of refrigeration is not vehicle specific. Factors such as service load, cold storage temperature and storage volume are required to calculate refrigeration load and therefore refrigeration cost. Also vehicle refrigeration will not always operate at full load and therefore a direct comparison cannot be made to traction costs. Figure 30 shows the running costs of refrigeration per hour of pure VC systems and dual stage sorption-VC systems (T_{inter} = 5°C). It can be seen that a vast cost saving can be achieved using a dual stage system however these systems are very large and heavy, which will reduce to vehicle space and also the increase fuel consumption and reduce vehicle performance.

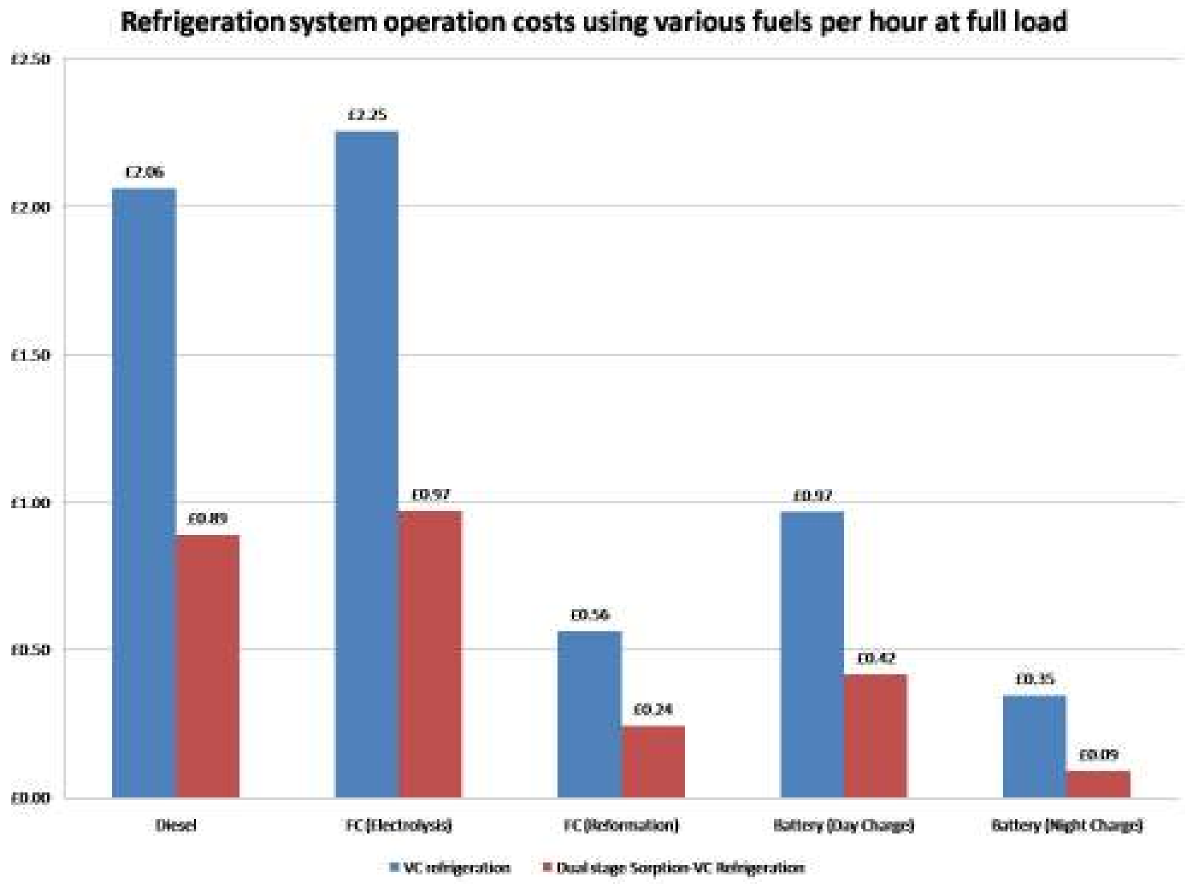

Figure 30 – Refrigeration costs using various fuels per hour

Again the most expensive running cost is experienced by fuel cells using hydrogen from electrolysis and the cheapest is battery technology. As stated, fuel cell systems are the best as these eliminate the issues of batteries and are also lighter which means that these systems cannot affect vehicle performance and fuel consumption.

Capital cost model has not been conducted in this report as such a comparison is not valid as fuel cells are current in research stage where as ICE and battery technologies are highly mature. Such a capital cost will be conducted on future fuel cell predictions based on volume sales, however this project would be used as a demonstration system to highlight the benefits of such technology today.

6. Conclusions

From the literature review FCHEVs show great potential and have several benefits over other technologies:

- Zero carbon emissions, little/no noise and vibration compared with ICEs
- Greater efficiencies which are not limited to Carnot efficiency like ICEs
- Hydrogen can be produced from green sources and a renewable sources unlike fossil fuels
- Hydrogen has a greater energy density compared to battery technology
- Quick refuelling time and no dependency on electricity grid compared with battery vehicles
- Reduce battery weight in a hybridised system

From reviewing refrigeration technologies, VC and sorption refrigeration are the most viable solutions for onboard refrigeration. Onboard refrigeration incorporated into the vehicle traction system by either using an electric motor to power a VC system or the waste heat produced from the fuel cell reaction can be used to power a sorption refrigeration system. However the temperatures produced by PEMFCs are low in comparison to the high temperatures required at the generator of sorption systems capable of producing freezing temperatures. Therefore a dual stage sorption-VC system is required. Current commercially available onboard refrigeration systems do not use the waste heat from diesel engines however research has been conducted to assess the feasibility of this.

Modelling in this thesis has shown that using the waste heat from the fuel cell reaction can greatly reduce compressor power and increase COP of the VC system in a dual stage system.

As a result such system will have lower running costs in comparison with pure VC onboard systems. However for such systems to operate, the heat generated from the fuel cell and therefore the power drawn must be steady. During the vehicle drive cycle analysis conducted in this thesis, it can be seen that the fuel cell does not operate at a constant power and therefore will not generate constant heat. In addition sorption systems have a low COP, however this does not have a effect as the heat used is a biproduct of the fuel cell reaction which is not normally used. Sorption systems are also very large and heavy which do not make them suitable for delivery vehicles where space is the key requirement. Research is being conducted to reduce the size and weight of sorption refrigeration systems.

Vehicle modelling has shown that the hybridisation factor must be tailored to ensure the efficient operation of the fuel cell. The energy consumption of 0.1 or below for HGVs shows the fuel cell energy consumption to increase. Hybridisation above 0.7 there is little difference in energy consumption however the literature review has highlighted that this region is highly inefficient. Further work is needed on vehicle modelling to analyse the effect of vehicle weight and size on efficiency and hydrogen fuel consumption.

Cost modelling has shown that the BEVs have the lower running costs from both traction and refrigeration. However these vehicles have several shortcomings as discussed which are eliminated by FCHEVs. Also additional weight will reduce performance and increase fuel consumption. FCHEVs using regenerative braking, purified reformed hydrogen and use off peak electricity have several system advantages at a very small increase in cost compared with BEVs.

7. Further Work

Further work includes:

1. Model and analyse the efficiency and fuel consumption of HGVs at various levels of hybridisation and vehicle weights
2. Investigate the use of PEMFCs or HT-PEMFCs in refrigerate vehicles
3. Produce a bench prototype of an VC and a dual stage sorption-VC onboard refrigeration system powered by a fuel cell hybrid system
4. Review and produce an onboard refrigeration control strategy to improve refrigeration system efficiency using a fuel cell hybrid system

8. Appendix

8.1 Raw reviewed refrigeration unit data

Table 11 - Trailer Refrigeration Unit Data [8]

Manufacturer	Unit Name	Engine Name	Engine Power (W)	Cooling Capacity (38°C Ambient)		Fuel Consump. (l/h)	Carbon Emissions (kg/h)	COP (37% thermal efficiency)	
				0°C	18°C			0°C	18°C
Thermoking	Spectrum SB	TK486V	25400	13188	8499	2.62	7.07	1.40	0.90
Thermoking	Spectrum DE	TK485	25400	14950	9085	2.62	7.07	1.59	0.97
Thermoking	SB-400	TK486	25400	17585	11723	2.62	7.07	1.87	1.25
Thermoking	SB-330	TK487	25400	18756	10843	2.62	7.07	2.00	1.15
Thermoking	SB-230	TK488	25400	14950	9380	2.62	7.07	1.59	1.00
Thermoking	SB-200TG	TK486V	25400	14950	9380	2.62	7.07	1.59	1.00

Table 12 - Truck Refrigeration Unit data [8]

Manufacturer	Unit Name	Engine Name	Engine Power (W)	Cooling Capacity (38°C Ambient)		Fuel Consump. (l/h)	Carbon Emissions (kg/h)	COP (37% thermal efficiency)	
				0°C	18°C			0°C	18°C
Thermoking	MD-100	TK380	8948.4	3223	2403	0.92	2.49	0.97	0.73
Thermoking	T-600R	TK370	11185.5	5860	3809	1.15	3.11	1.42	0.92
Thermoking	T-600	TK371	11185.5	5860	3809	1.15	3.11	1.42	0.92
Thermoking	T-800R	TK372	11185.5	5860	3663	1.15	3.11	1.42	0.89
Thermoking	T-800	TK373	11185.5	7179	4395	1.15	3.11	1.73	1.06
Thermoking	T-1000R	TK376	14615.7	7032	4845	1.51	4.07	1.30	0.90
Thermoking	T-1000	TK377	14615.7	9962	6153	1.51	4.07	1.84	1.14
Thermoking	UT-1200X	TK378	14615.7	10138	6534	1.51	4.07	1.87	1.21

Table 13 - Direct drive refrigeration unit data using a reverse calculation (Small - Medium sized vans and box type trucks) [8, 74]

Manufacturer	Unit Name	Cooling Capacity (38°C Ambient)		Power Input (W)		Engine power (assuming 37% efficiency)		Fuel Comsump. (l/h)		Carbon Emissions (kg/h)	
		0	-18	H COP	L COP	H COP	L COP	H COP	L COP	H COP	L COP
Thermoking	V-200 Max	2098	1399	1249.11	1706.10	3375.97	4611.07	0.35	0.48	0.94	1.28
Thermoking	V-300 Max	2934	1710	1526.79	2085.37	4126.45	5636.12	0.43	0.58	1.15	1.57
Thermoking	V-520 Max	4864	2549	2275.89	3108.54	6151.06	8401.45	0.63	0.87	1.71	2.34
Thermoking	V-700 Max	6010	3370	3008.93	4109.76	8132.24	11107.45	0.84	1.15	2.26	3.09
Manufacturer	**Unit Name**	**Cooling Capacity (30°C Ambient)**		**Power Input (W)**		**Engine power (assuming 37% efficiency)**		**Fuel Comsump. (l/h)**		**Carbon Emissions (kg/h)**	
		0	-18	H	L	H	L	H	L	H	L
Hubbard	460 Alpha	3360	1850	1651.79	2256.10	4464.29	6097.56	0.46	0.63	1.24	1.70
Hubbard	480 Alpha	3360	1800	1607.14	2195.12	4343.63	5932.76	0.45	0.61	1.21	1.65
Hubbard	390 AlphaL/EL	2700	1750	1562.50	2134.15	4222.97	5767.96	0.44	0.59	1.18	1.61
Hubbard	500 Alpha	4000	2200	1964.29	2682.93	5308.88	7251.15	0.55	0.75	1.48	2.02
Hubbard	520 Alpha	4990	2950	2633.93	3597.56	7118.73	9723.14	0.73	1.00	1.98	2.71
Hubbard	720 Alpha	6830	3340	2982.14	4073.17	8059.85	11008.57	0.83	1.13	2.24	3.06

8.2 Examples of refrigeration model

8.2.1 Vehicle cooling requirement model

Vehicle Cooling Requirement Model		
Vehicle Storage dimensions (Without insulation)		
Width	2.5	m
Length	4	m
Height	2.5	m
Volume	25	m3
Surface area	52.5	m2
Insulation		
Thickness	0.05	m
k value	0.022	WmK
Temperature Requirements		
Tamb	38	C
Tveh	-20	C
dT	58	C
Amended dimensions		
Width	2.4	m
Length	3.9	m
Depth	2.4	m
Volume	22.464	m3
Surface area	48.96	m2

Q loss through insulation		
Average surface area	50.73	m2
Qinsulation	1294.63	W
Factor for leaks	1.5	
Qinsulation total	1941.944	W
Q service load		
Number of door openings	3	
Duration per opening	4	
Service load	2.17	w/m3/c
Q service load	2827.319	W
Q total	4769.263	W

	Opening Duration (Mins)					
Door openings per hours	3	4	5	6	7	8
1	0.61	0.62	0.63	0.64	0.66	0.67
2	1.29	1.34	1.39	1.45	1.51	1.58
3	2.04	2.17	2.31	2.4	2.67	2.89
4	2.89	3.15	3.47	3.86	4.34	Impractical
5	3.86	4.34	4.96	5.79	Impractical	Impractical
6	4.96	5.78	6.94	Impractical	Impractical	Impractical
7	6.23	7.59	Impractical	Impractical	Impractical	Impractical
8	7.71	9.92	Impractical	Impractical	Impractical	Impractical
9	9.46	Impractical	Impractical	Impractical	Impractical	Impractical
10	11.57	Impractical	Impractical	Impractical	Impractical	Impractical
	Opening Duration (Mins)					
Door openings per hour	3	4	5	6	7	8
3	2.04	2.17	2.31	2.4	2.67	2.89

8.2.2 Vehicle vapour compression model

Vehicle Vapour Compression Model		
Cooling capacity requirement	4769.263	W
Factor	1	
Cooling capacity of ref system	4769.263	W
Base case		
Tamb	38	C
Tveh	-18	C
dT	56	C
Maximum COP	4.553571	
Actual COP	0.97	
COP factor	0.21302	
VC Refrigeration system		
Tamb	38	C
Tveh	-20	C
dT	58	C
Maximum COP	4.362069	
Actual COP	0.920397	
Compressor work	5181.748	W
Heat rejection at condenser	9951.012	W

8.2.3 Dual stage sorption-VC refrigeration model

Dual Stage Sorption VC Model		
Cooling capacity of ref system	4769.263	W
Base case (sorption)		
Tamb	38	C
Tveh	10	C
dT	28	C
Maximum COP	10.10714	
Actual COP	0.7	
COP factor	0.069258	
Tamb	38	C
Sorption Evap temperature	5	C
VC requirement		
Tveh	-20	C
dT	25	C
Maximum COP	10.12	
COP factor	0.211	
Actual COP	2.13532	
Compressor work	2233.512	
Heat rejection at condenser	7002.776	
Sorption Requirement		
Maximum COP	8.424242	
Actual COP	0.421212	
Q Evaporator	7002.776	W

Q Generator	16625.29	W

8.3 Examples of vehicle model

8.3.1 NEDC model

Mass of vehicle	5000.00	
Drag Coeff	0.5	
Density of air	1.2	kg/m3
Frontal Area	7	m2

u0	0.015
u1	7.00E-06
g	9.81

Power	Energy	
Max Power	No Regen	Regen
161315.7	6045.748422	5084.609

Time /s	Vehicle speed /km/h	Vehicle speed /m/s	Vehicle accel. /m/s2	Force due to accel. /N	Drag force /N	Rolling coeff	Roll force /N	Distance /m	Energy /J	Power/ W	Energy (No Regen) /Wh	Energy (Regen) /Wh
8	0	0	0	0	0	0.015	735.75	0	0	0	0	0
9	0	0	0	0	0	0.015	735.75	0	0	0	0	0
10	0	0	0	0	0	0.015	735.75	0	0	0	0	0
11	0	0	0	0	0	0.015	735.75	0	0	0	0	0
12	3.8	1.055556	1.055556	5277.778	2.339815	0.015008	736.1326	1.055556	6350.486	6350.486	1.764023964	1.764024
13	7.5	2.083333	1.027778	5138.889	9.114583	0.01503	737.2402	3.138889	12260.92	12260.92	3.40581233	3.405812
14	11.3	3.138889	1.055556	5277.778	20.69051	0.015069	739.1329	6.277778	18951.36	18951.36	5.264266466	5.264266
15	15	4.166667	1.027778	5138.889	36.45833	0.015122	741.7109	10.44444	24654.41	24654.41	6.848446944	6.848447
16	15	4.166667	0	0	36.45833	0.015122	741.7109	14.61111	3242.372	3242.372	0.900658878	0.900659
17	15	4.166667	0	0	36.45833	0.015122	741.7109	18.77778	3242.372	3242.372	0.900658878	0.900659
18	15	4.166667	0	0	36.45833	0.015122	741.7109	22.94444	3242.372	3242.372	0.900658878	0.900659
19	15	4.166667	0	0	36.45833	0.015122	741.7109	27.11111	3242.372	3242.372	0.900658878	0.900659
20	15	4.166667	0	0	36.45833	0.015122	741.7109	31.27778	3242.372	3242.372	0.900658878	0.900659
21	15	4.166667	0	0	36.45833	0.015122	741.7109	35.44444	3242.372	3242.372	0.900658878	0.900659

22	15	4.166667	0	0	36.45833	0.015122	741.7109	39.61111	3242.372	3242.372	0.900658878	0.900659
23	15	4.166667	0	0	36.45833	0.015122	741.7109	43.77778	3242.372	3242.372	0.900658878	0.900659
24	12	3.333333	-0.83333	-4166.67	23.33333	0.015078	739.565	47.11111	-11345.9	0	0	-3.15164
25	9	2.5	-0.83333	-4166.67	13.125	0.015044	737.8959	49.61111	-8539.11	0	0	-2.37198
26	6	1.666667	-0.83333	-4166.67	5.833333	0.015019	736.7038	51.27778	-5706.88	0	0	-1.58525
27	3	0.833333	-0.83333	-4166.67	1.458333	0.015005	735.9884	52.11111	-2857.68	0	0	-0.7938
28	0	0	-0.83333	-4166.67	0	0.015	735.75	52.11111	0	0	0	0

8.3.2 NEDC simulation of hybrid vehicle

Total power	161315.7407
Regen eff	0.5
Vehicle power	162000
Hybridisation	0.33
Battery power	53460
Fuel Cell power	108540

Time/ s	Power /W	Regen power with eff. /W	positive bat power /W	Total battery power /W	Remainder power above battery power /W	**Fuel cell power /W**	Remainder power above fuel cell power /W	**Total battery power /W**	Fuel Cell energy /Wh	Battery energy /Wh
5	0	0	0	0	0	0	0	0	0	0
6	0	0	0	0	0	0	0	0	0	0
7	0	0	0	0	0	0	0	0	0	0
8	0	0	0	0	0	0	0	0	0	0
9	0	0	0	0	0	0	0	0	0	0
10	0	0	0	0	0	0	0	0	0	0
11	0	0	0	0	0	0	0	0	0	0
12	6350.486272	0	6350.486272	6350.486272	0	0	0	6350.486	0	1.764024
13	12260.92439	0	12260.92439	12260.92439	0	0	0	12260.92	0	3.405812
14	18951.35928	0	18951.35928	18951.35928	0	0	0	18951.36	0	5.264266
15	24654.409	0	24654.409	24654.409	0	0	0	24654.41	0	6.848447
16	3242.371962	0	3242.371962	3242.371962	0	0	0	3242.372	0	0.900659
17	3242.371962	0	3242.371962	3242.371962	0	0	0	3242.372	0	0.900659

18	3242.371962	0	3242.371962	3242.371962	0	0	0	3242.372	0	0.900659
19	3242.371962	0	3242.371962	3242.371962	0	0	0	3242.372	0	0.900659
20	3242.371962	0	3242.371962	3242.371962	0	0	0	3242.372	0	0.900659
21	3242.371962	0	3242.371962	3242.371962	0	0	0	3242.372	0	0.900659
22	3242.371962	0	3242.371962	3242.371962	0	0	0	3242.372	0	0.900659
23	3242.371962	0	3242.371962	3242.371962	0	0	0	3242.372	0	0.900659

8.4 Examples of cost model

8.4.1 Vehicle cost model

Single Power Source Vehicle				**Cost**		
Total Vehicle Energy	6045.75	Wh		Diesel	1.40	£/l
				Hydrogen (electrolysis)	5.16	£/kg
Hybridised Vehicle using Regen				Hydrogen (Reformation)	1.29	£/kg
Total Energy	5565.18	Wh		Cost of Electricity (Day)	0.14	£/kWh
Primary Energy	2636.7379	Wh		Cost of Electricity (Night)	0.05	£/kWh
Battery Energy	2928.44	Wh				
				Efficiencies		
Non Refrigerated vehicles				Diesel Engine	0.37	
Diesel Engine				Diesel Engine fuel conversion	0.98	
Engine energy required	16673.33	Wh		Fuel Cell	0.50	
Fuel consumption	1.72	l		Fuel Cell fuel conversion	0.95	
				Electric motor	0.75	
Total cost	2.41	£				
Diesel Engine Hybrid				Diesel Engine	£2.41	
Primary Energy	7271.75	Wh		Diesel Hybrid (Day Charge)	£1.60	
Fuel Consumption	0.75	l		Diesel Hybrid (Night Charge)	£1.24	
Cost of Diesel	1.05	£		Pure Battery (Day Charge)	£1.04	
Battery Energy	3904.59	Wh		Pure Battery (Night Charge)	£0.37	
Cost of Electricity (Day)	0.55	£		Fuel Cell (Electrolysis)	£2.63	
Cost of Electricity (Night)	0.20	£		Fuel Cell (Reformation)	£0.66	
				FCHEV (Electrolysis + Day Charge)	£1.69	
Total cost (Day Charge)	1.60	£		FCHEV (Reformation + Day Charge)	£0.83	
Total cost (Night Charge)	1.24	£		FCHEV (Electrolysis + Night Charge)	£1.34	

				FCHEV (Reformation + Night Charge)	£0.48	
Pure Battery				FCHEV (Electrolysis)	£1.15	
Battery Energy	7420.24	Wh		FCHEV (Reformation)	£0.29	
Total cost (Day Charge)	1.04	£				
Total cost (Night Charge)	0.37	£				
Pure Fuel Cell						
Fuel Cell Energy	16970.52	Wh				
Hydrogen consumption	0.51	kg				
Total Cost (Electrolysis)	2.63	£				
Total Cost (Reformation)	0.66	£				
Fuel Cell Hybrid						
Fuel Cell Energy	7401.37	Wh				
Hydrogen consumption	0.22	kg				
Total Cost (Electrolysis)	1.15	£				
Total Cost (Reformation)	0.29	£				
Battery Energy	3904.59					
Cost of Electricity (Day)	0.55	£				
Cost of Electricity (Night)	0.20	£				
Total Cost (Electrolysis + Day Charge)	1.69					
Total Cost (Reformation + Day Charge)	0.83					
Total Cost (Electrolysis + Night Charge)	1.34					
Total Cost (Reformation + Night Charge)	0.48					

8.4.2 Refrigeration cost model

Refrigeration Energy				**Cost**		
Vehicle Refrigeration (VC)	5181.75	Wh		Diesel	1.40	£/l
Dual stage at 5C intermediate temp	2233.51	Wh		Hydrogen (electrolysis)	5.16	£/kg
				Hydrogen (Reformation)	1.29	£/kg
				Cost of Electricity (Day)	0.14	£/kWh
Pure VC				Cost of Electricity (Night)	0.05	£/kWh
Diesel						
VC Energy	14290.54	Wh		**Efficiencies**		
Litres of diesel	1.47	l		Diesel Engine	0.37	
				Diesel Engine fuel conversion	0.98	
Total cost	2.06	£		Fuel Cell	0.50	
				Fuel Cell fuel conversion	0.95	
Pure fuel cell				Electric motor	0.75	
Energy	14545.26	Wh				
kg of hydrogen	0.44	kg		Diesel	£2.06	£0.89
				FC (Electrolysis)	£2.25	£0.97
Total cost (Electrolysis)	2.25	£		FC (Reformation)	£0.56	£0.24
Total cost (Reformation)	0.56	£		Battery (Day Charge)	£0.97	£0.42
				Battery (Night Charge)	£0.35	£0.09
Battery						
Energy	6909.00	Wh				
Total cost (Day charge)	0.97	£				
Total cost (Night charge)	0.35	£				
Dual stage						
Diesel						

Energy	6159.71	Wh				
Litre of diesel	0.64	l				
Total Cost	0.89	£				
Fuel cell						
Energy	6269.51	Wh				
hydrogen	0.19	kg				
Total cost (Electrolysis)	0.97	£				
Total cost (Reformation)	0.24	£				
Battery						
Energy	2978.02	Wh				
Total cost (Day charge)	0.42	£				
Total cost (Night charge)	0.09	£				

References

1. DEFRA, *The Validity of Food Miles as an Indicator of Sustainable Development: Final Report ED50254*. 2005.
2. von Helmolt, R. and U. Eberle, *Fuel cell vehicles: Status 2007.* Journal of Power Sources, 2007. **165**(2): p. 833-843.
3. BP (2011) *BP Statistical Review of World Energy June 2011*.
4. Transport, D.f. *Rates of Vehicle Tax - V149*.
5. EU. *Low Emission Zones in Europe*. [cited 2011 27/01/11]; Available from: http://www.lowemissionzones.eu/.
6. ACEA, *Commercial Vehicles and CO2*. 2010, ACEA.
7. Schoemaker, J., *PIEK-Programme (The Netherlands)*. 2005, Osmose.
8. Thermoking. *Products*. 2011 [cited 2011 26/5/2011]; Available from: http://www.thermoking.com/tk/index.asp?region=euromideafrica.
9. Transicold, C. *New Unit Enables Night Deliveries with Standard Installation*. 2011 [cited 2011 26/5/2011]; Available from: http://www.carriertransicoldeurope.com/ml/news/news_niv2.php?area=4&sites=3&lang=en&id_news=150.
10. Pilatte, A., *Refrigeration Fundamentals*. 2005, International Institute of Refrigeration: Belgium.
11. Dincer, I. and M. Kanoglu, *Refrigeration Systems and Applications*. 1st ed. 2010: John Wiley & Sons Ltd.
12. ASHRAE, *2010 ASHRAE Handbook Refrigeration - Inch-Pound Edition*. 2010: American Society of Heating, Refrigerating and Air-Conditioning Engineers.
13. Wang, R.Z. and R.G. Oliveira, *Adsorption refrigeration--An efficient way to make good use of waste heat and solar energy.* Progress in Energy and Combustion Science, 2006. **32**(4): p. 424-458.
14. Tassou, S.A., et al., *A review of emerging technologies for food refrigeration applications.* Applied Thermal Engineering, 2010. **30**(4): p. 263-276.
15. Unilever, *Good Ice Cream Cold Chain Practice (GICCCP)*, in *Supply Chain*. 2007: Vlaardingen. p. 4.
16. Hong, D., et al., *A novel absorption refrigeration cycle.* Applied Thermal Engineering, 2010. **30**(14-15): p. 2045-2050.
17. Solair. *Adsorption Chillers*. 2009 [cited 2011 26/5/2011]; Available from: http://www.solair-project.eu/142.0.html.
18. Technology, C.R. (2010) *Guide to ATP for Road Hauliers and Manufacturers*.
19. T. D. Eastop, A.M., *Applied Thermodynamics for Engineering Technologists*. 5th ed. 1993: Pearson Education Limited.
20. Tassou, S.A., G. De-Lille, and Y.T. Ge, *Food transport refrigeration - Approaches to reduce energy consumption and environmental impacts of road transport.* Applied Thermal Engineering, 2009. **29**(8-9): p. 1467-1477.
21. Ltd, B.P. *New Pallets*. 2011 [cited 2011 3/6/2011]; Available from: http://www.bridgwaterpallets.com/html/new_pallets.html.
22. Pulkrabek, W.W., *Engineering Fundamentals of the Internal Combustion Engine*. 2nd ed. 2003: Prentice Hall.
23. Goering, C.E., *Compression Ignition Engines*, in *Off-Road Vehicle Engineering Principles*. 2003, ASAE.
24. Wong, J.Y., *Theory of Ground Vehicles*. 3rd ed. 2001: John Wiley & Sons Inc.

25. Garrett, T.K., K. Newton, and W. Steeds, *The Motor Vehicle*. 12th Edition ed. 2000: Butterworth Heinemaan.
26. Labeckas, G. and S. Slavinskas, *Comparative performance of direct injection diesel engine operating on ethanol, petrol and rapeseed oil blends.* Energy Conversion and Management, 2009. **50**(3): p. 792-801.
27. Mårtensson, L., *Emissions from Volvo Trucks.* 2006.
28. Company, F.M. (2011) *Ford Transit Van*.
29. (UK), D.f.T., *Buyers Guide to Refrigerated Transport Equipment*. 2007.
30. Craig Christy, R.T., *Adsorption Air-Conditioning for Containerships and Vehicles - Final Report 00-07*. 2004, California State University Long Beach.
31. Manzela, A.A., et al., *Using engine exhaust gas as energy source for an absorption refrigeration system.* Applied Energy, 2010. **87**(4): p. 1141-1148.
32. Hubbard (2011) *Keep It Cool - A Guide To Transport Refrigeration*.
33. Unilever, *USA Q1 2011 Transport CO2 data collection*, Unilever, Editor. 2011.
34. Directgov. *Speed limits and speeding*. 2011 [cited 2011 29/7/11]; Available from: http://www.direct.gov.uk/en/TravelAndTransport/Roadsafetyadvice/DG_178867?CID=TAT&PLA=url_mon&CRE=speed_limits.
35. DoE, U.S., *Fuel Cell Handbook 7*. 2004, U.S Department of Energy: Morgantown, West Virginia.
36. Larminie, J., Dicks, A., *Fuel Cell Systems Explained*. 2nd Edition ed. 2003: John Wiley & Sons Ltd.
37. Guo, L.J., et al., *Solar hydrogen production and its development in China.* Energy, 2009. **34**(9): p. 1073-1090.
38. Su, H., et al., *Hydrogen production from water hyacinth through dark- and photo-fermentation.* International Journal of Hydrogen Energy, 2010. **35**(17): p. 8929-8937.
39. Zhang, H., G. Lin, and J. Chen, *Evaluation and calculation on the efficiency of a water electrolysis system for hydrogen production.* International Journal of Hydrogen Energy, 2010. **35**(20): p. 10851-10858.
40. Zhang, J., et al., *High temperature PEM fuel cells.* Journal of Power Sources, 2006. **160**(2): p. 872-891.
41. Courtney, J.M., *Bio-Engineered Gas Diffusion Electrodes (GDEs) for Proton Exchange Membrane Fuel Cells (PEMFCs)*, in *Chemical Engineering*. 2010, University of Birmingham: Birmingham.
42. Wu, D.W. and R.Z. Wang, *Combined cooling, heating and power: A review.* Progress in Energy and Combustion Science. **32**(5-6): p. 459-495.
43. Fuhs, A.E., *Hybrid Vehicles and The Future of Personal Transportation*. 2009: CRC Press.
44. Gigliucci, G., et al., *Demonstration of a residential CHP system based on PEM fuel cells.* Journal of Power Sources, 2004. **131**(1-2): p. 62-68.
45. Sinha, J., *Direct Hydrogen PEMFC Manufacturing Cost*, in *2009 DOE Hydrogen Program Revie*, U.S. DoE, Editor. 2009: Arlington, VA.
46. Jayanti Sinha, J.M., Katie Randolph, Thomas G. Benjamin, *FY 2010 Annual Progress Report - Cost Analysis of Fuel Cell Stack/Systems*, in *DOE Hydrogen Program*. 2010.
47. Krishnan, P., J.-S. Park, and C.-S. Kim, *Performance of a poly(2,5-benzimidazole) membrane based high temperature PEM fuel cell in the presence of carbon monoxide.* Journal of Power Sources, 2006. **159**(2): p. 817-823.
48. Bonville, L.J., et al., *Development and demonstration of a higher temperature PEM fuel cell stack.* Journal of Power Sources, 2005. **144**(1): p. 107-112.

49. Jayanti Sinha, S.L., Yong Yang, *Direct Hydrogen PEMFC Manufacturing Cost Estimation for Automotive Applications - 2009 DOE Hydrogen Program Review*. 2009, TIAX LLC: Cambridge.
50. Harry A. Dwyer, J.G., Walt Podolski, *FY 2005 Progress Report - VII.K.5 Demonstration and Evaluation of Fuel Cell Powered Trailer Refrigeration Units (TRUs)*. 2005.
51. CJ Brodrick, H.A.D., *2005 DOE Hydrogen ProgramFuel Cell APU*. 2005, University of California, ITS, Davis.
52. Acres, G.J.K., *Recent advances in fuel cell technology and its applications.* Journal of Power Sources, 2001. **100**(1-2): p. 60-66.
53. Offer, G.J., et al., *Techno-economic and behavioural analysis of battery electric, hydrogen fuel cell and hybrid vehicles in a future sustainable road transport system in the UK.* Energy Policy, 2011. **39**(4): p. 1939-1950.
54. Fischer, M., M. Werber, and P.V. Schwartz, *Batteries: Higher energy density than gasoline?* Energy Policy, 2009. **37**(7): p. 2639-2641.
55. Jeong, K.S. and B.S. Oh, *Fuel economy and life-cycle cost analysis of a fuel cell hybrid vehicle.* Journal of Power Sources, 2002. **105**(1): p. 58-65.
56. Chalk, S.G. and J.F. Miller, *Key challenges and recent progress in batteries, fuel cells, and hydrogen storage for clean energy systems.* Journal of Power Sources, 2006. **159**(1): p. 73-80.
57. Jazar, R.N., *Vehicle Dynamics Theory and Application*. 2008: Springer Science and Business Media, LLC.
58. Grid, N. *Ten Year Statement - National Grid UK Plans*. 2011; Available from: http://www.nationalgrid.com/uk/Gas/TYS/.
59. Toshiba. *Super-Charge Ion Battery (SCiB™)*. 2011; Available from: http://www.toshiba.com/ind/product_display.jsp?id1=821.
60. K. Wipke, S.S., J. Kurtz, J. Garbak, *Fuel Cell Vehicle Infrastructure Learning Demonstration: Status and Results*. 2008, National Renewable Energy Laboratory.
61. Henne, R.H. and K.A. Friedrich, *APPLICATIONS - TRANSPORTATION | Auxiliary Power Units: Fuel Cells*, in *Encyclopedia of Electrochemical Power Sources*, x00Fc and G. rgen, Editors. 2009, Elsevier: Amsterdam. p. 157-173.
62. Margalef, P. and S. Samuelsen, *Integration of a molten carbonate fuel cell with a direct exhaust absorption chiller.* Journal of Power Sources, 2010. **195**(17): p. 5674-5685.
63. Pilatowsky, I., et al., *Simulation of an air conditioning absorption refrigeration system in a co-generation process combining a proton exchange membrane fuel cell.* International Journal of Hydrogen Energy, 2007. **32**(15): p. 3174-3182.
64. Zhang, X., et al., *A review of integration strategies for solid oxide fuel cells.* Journal of Power Sources, 2010. **195**(3): p. 685-702.
65. Zink, F., Y. Lu, and L. Schaefer, *A solid oxide fuel cell system for buildings.* Energy Conversion and Management, 2007. **48**(3): p. 809-818.
66. Staffell, I. and A. Ingram, *Life cycle assessment of an alkaline fuel cell CHP system.* International Journal of Hydrogen Energy, 2010. **35**(6): p. 2491-2505.
67. Zhang, X., et al., *Maximum equivalent efficiency and power output of a PEM fuel cell/refrigeration cycle hybrid system.* International Journal of Hydrogen Energy, 2011. **36**(3): p. 2190-2196.
68. DieselNet. *Emission Test Cycles*. 2012 [cited 2012 29/07/12]; Available from: http://www.dieselnet.com/standards/cycles/ece_eudc.php.
69. Shaughnessy, E.J., I.M. Katz, and J.P. Schaffer, *Introduction to Fluid Mechanics*. 1st ed. 2005: Oxford University Press.

70. Factbook, P. *Energy Density of Hydrogen*[*http://hypertextbook.com/facts/2005/MichelleFung.shtml*](http://hypertextbook.com/facts/2005/MichelleFung.shtml). 2005 [cited 2012 29/07/12].
71. Bolton, P. (2012) *Petrol and diesel prices*. Social and General Statistics.
72. Heptonstall, P. (2007) *A Review of Electricity Unit Cost Estimates*.
73. energy, c.a. *Fuel Prices*. 2012 [cited 29/07/12 2012]; Available from: http://www.confusedaboutenergy.co.uk/index.php/domestic-fuels/fuel-prices.
74. Hubbard. [cited 2011 27/01/11]; Available from: http://www.hubbard.co.uk/.